Int. J. Solids Structures Vol. 26. No. 9/10, pp. 945–973, 1990
Printed in Great Britain.

0020–7683/90 $3.00+ .00

KOITER'S STABILITY THEORY IN A COMPUTER-AIDED ENGINEERING (CAE) ENVIRONMENT†

J. ARBOCZ and J. M. A. M. HOL
Delft University of Technology, The Netherlands

Abstract—The development of "DISDECO", the Delft Interactive Shell Design Code is described. The purpose of this project is to make the accumulated theoretical, numerical and practical knowledge of the last 20 years readily accessible to users interested in the analysis of buckling sensitive structures. With this open ended, hierarchical, interactive computer code the user can access from his work-station successive programs of increasing complexity.

Included are modules that contain Koiter's imperfection sensitivity theory extended to anisotropic shell structures under combined loading. The nonlinear Donnell-type anisotropic shell equations in terms of the radial displacement W and the Airy stress function F are used. The circumferential dependence is eliminated by Fourier decomposition. The resulting sets of ordinary differential equations are solved numerically via the "Shooting Method". Thus the specified boundary conditions can be enforced rigorously not only in the pre-buckling but also in the buckling and post-buckling problem. Initial results indicate that in order to obtain reliable results for anisotropic shells rigorous enforcing of the edge restraint and of the boundary conditions is indeed a must.

1. INTRODUCTION

The central goal of the current shell research activities at the Faculty of Aerospace Engineering of the TU-Delft is the development of "Improved Shell Design Criteria" for buckling sensitive structures, which incorporate all the theoretical knowledge accumulated in the last, say, 30 years through intensive research in the Aerospace, the Nuclear and the Offshore fields and which make efficient use of the currently available interactive and (super) computing facilities.

All the current design manuals (Weingarten *et al.*, 1965; Anonymous, 1977; Anonymous, 1980) adhere to the so-called "Lower Bound Design Philosophy" that was already in use 50 years ago. That is, they recommend the use of an empirical "knockdown" factor γ, which is so chosen that when it is multiplied with the (classical) buckling load of the perfect shell a "lower bound" to all available data is obtained (see Fig. 1).

The improvements in the currently recommended shell design procedures are primarily sought in a more selective approach to the choice of the "knockdown" factor γ. Due to the

† Presented at XVIIth International Congress of Theoretical and Applied Mechanics, 21–27 August 1988, Grenoble, France.

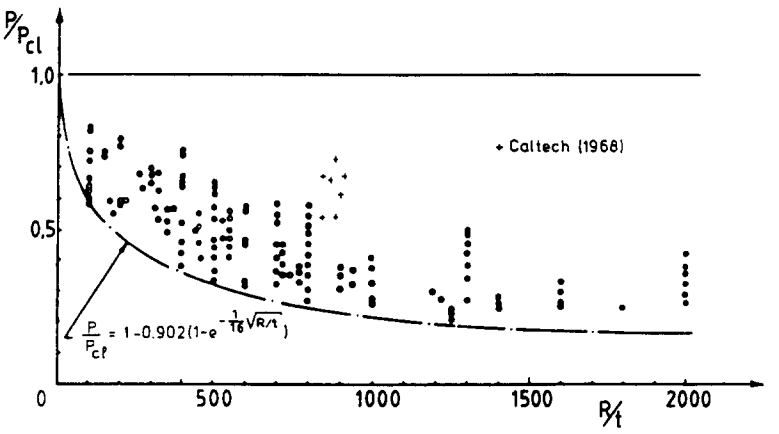

Fig. 1. Test data for isotropic cylinders under axial compression (Weingarten *et al.*, 1965).

pioneering efforts of Koiter (1945), Budiansky and Hutchinson (1964) and many other investigators, initial geometric imperfections have been identified as the main cause for the wide experimental scatter observed in practice. Thus it is proposed that if a company takes the necessary care to produce all its shells according to well characterized standards, and if it can show via experiments that the boundary conditions are defined in such a way that during assembly no additional imperfections (especially at the shell edges) are introduced, then the use of an improved (higher) "knockdown" factor γ derived by the stochastic approach proposed by Elishakoff and Arbocz (1985) and Elishakoff *et al.* (1987) should be allowed. The proposed new "Improved Shell Design Criteria" can be represented by the following formula

$$P_a \leqslant \frac{\lambda_a}{\text{F.S.}} P_c \tag{1}$$

where P_a = allowable buckling load, P_c = buckling load of the "perfect" structure calculated via one of the advanced shell codes like BOSOR-4 (Bushnell, 1972), λ_a = reliability based improved (higher) "knockdown" factor and F.S. = factor of safety.

The steps involved in the definition of the reliability based improved (higher) "knockdown" factor λ_a can be summarized as follows:

1. Compute the Fourier coefficients of the measured initial imperfection surveys of a relatively small sample (say four) nominally identical shells produced by the same manufacturing process.
2. Calculate by ensemble averaging the mean vector and the variance–covariance matrix of the Fourier coefficients of the experimental sample.
3. Use the First-Order Second-Moment Analysis (Elishakoff *et al.*, 1987) to compute the reliability function $R(\lambda)$ of the buckling of shells with general random imperfections.
4. Determine the improved (higher) "knockdown" factor λ_a for the specified reliability from the plot of $R(\lambda)$ vs λ, where λ is the normalized load parameter (see Fig. 2).

Notice that by using the First-Order Second-Moment Analysis to derive the reliability functions for shells produced by a certain manufacturing process, one is combining the Lower Bound Design Philosophy with the notion of Goodness Classes. Thus shells made by a process which produces inherently a less damaging initial imperfection distribution will not be penalized because of the lower experimental results obtained with shells produced by another process, which generates a more damaging characteristic initial imperfection distribution.

2. DEVELOPMENT OF "DISDECO"

The key to the success of any Stochastic Stability Analysis lies in the reliability and accuracy of the buckling load predictions made by the deterministic buckling analysis used.

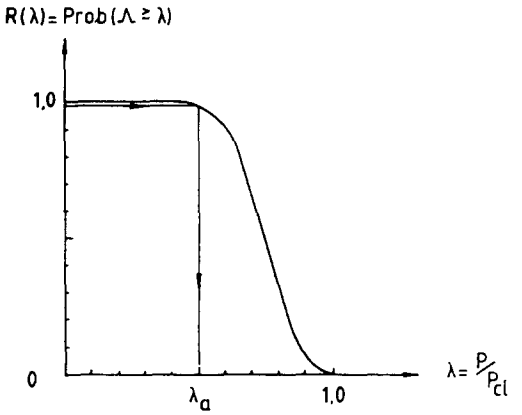

Fig. 2. Reliability function $R(\lambda)$ for a given R/t ratio.

On the other hand the success of the deterministic buckling load analysis depends very heavily on the appropriate choice of the nonlinear model employed, which in turn requires considerable knowledge by the analyst as to the expected physical behaviour of imperfect shell structures. As has been pointed out by Arbocz and Babcock (1980) this knowledge can best be acquired by first using the series of imperfection sensitivity analysis of increasing complexity that have been published in the literature.

In order to make the search for the most appropriate nonlinear model feasible the development of "DISDECO", the Delft Interactive Shell Design Code has been initiated. This "open architecture" interactive code will combine shell computer programs of different degrees of sophistication with the latest tools of information science such as Data Bases, Interactive Graphics and Expert Systems into an advanced hierarchical *design and analysis system*.

Analysing existing interactive systems for different types of applications has led to the identification of their major components. Based on the results of this study the conceptual design of the global architecture of DISDECO has been completed. The building blocks of the full scale system and their functional relations are displayed in Fig. 3.

The central part of the whole system is the "Command and Control Processor". Its function is to control and direct the activities of the system. It starts-up and winds-down the design system, processes user input through execution of modules, creates a working environment and in general is the working partner of the user.

The link from the user to the command and control processor passes through the "Man-Machine Interface". Assuming that the user employs a terminal device or work-station which supports graphics, the man-machine interface controls the input stream from the user, analyses it, checks it for correct syntax, validates the commands and passes it in an interpretable format to the command and control processor. In a similar manner the output stream from the design and analysis system is converted to a meaningful output for the user.

To increase the flexibility of DISDECO the dependence on a specific data management system must be minimized. Therefore, a "Generalized Database Interface" is needed to shield the global design and analysis system from the peculiarities of a commercially acquired RDBMS (Relational Data Base Management System).

The real work of DISDECO is done by a number of dedicated "Analysis Modules". Supplementary modules are required for pre- and post-processing functions, remote batch processing of analysis tasks and general utility functions. An essential supplementary module is dedicated to the provision of on-line help information about system capabilities, usage details and at a later stage for literature retrieval.

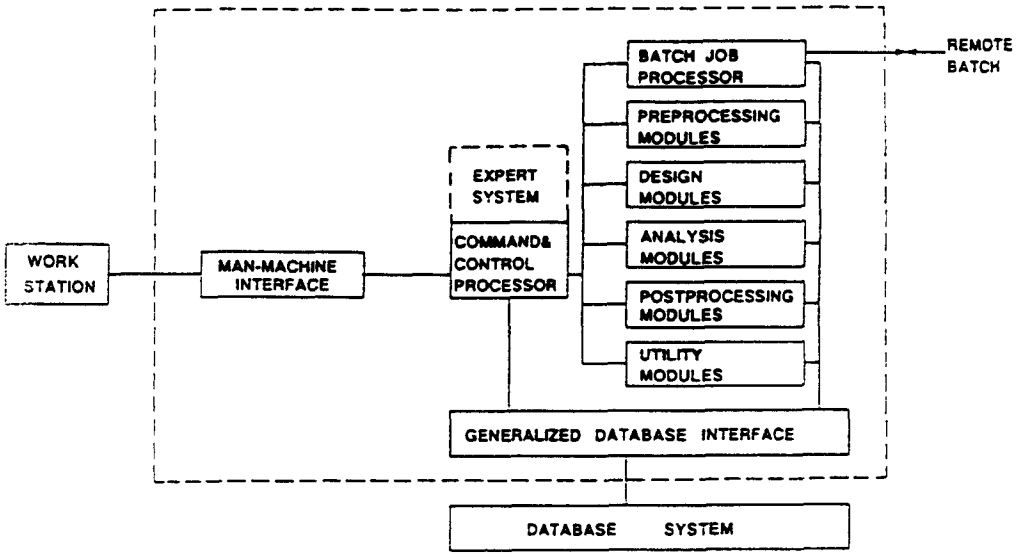

Fig. 3. Global architecture of the interactive shell design and analysis system "DISDECO".

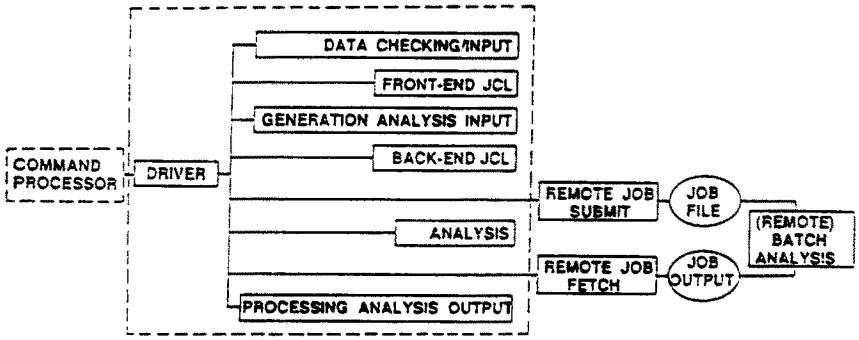

Fig. 4. Generalized analysis module.

Analysis modules can be of several types. Small analysis tasks can be done interactively under control of the design system, while large analysis tasks must be performed through batch processing either on the same computer or on a remote (super) computer. Medium size tasks can be done optionally interactively or through remote batch processing. This approach ensures optimum usage of available computing resources and frees the design system for other tasks. The layout of a generalized analysis module is shown in Fig. 4.

The development of the proposed design and analysis system DISDECO can only be concluded successfully through a step by step evolutionary effort. Thus initially a pilot system, containing the essential core features of the full scale system shown in Fig. 5, has

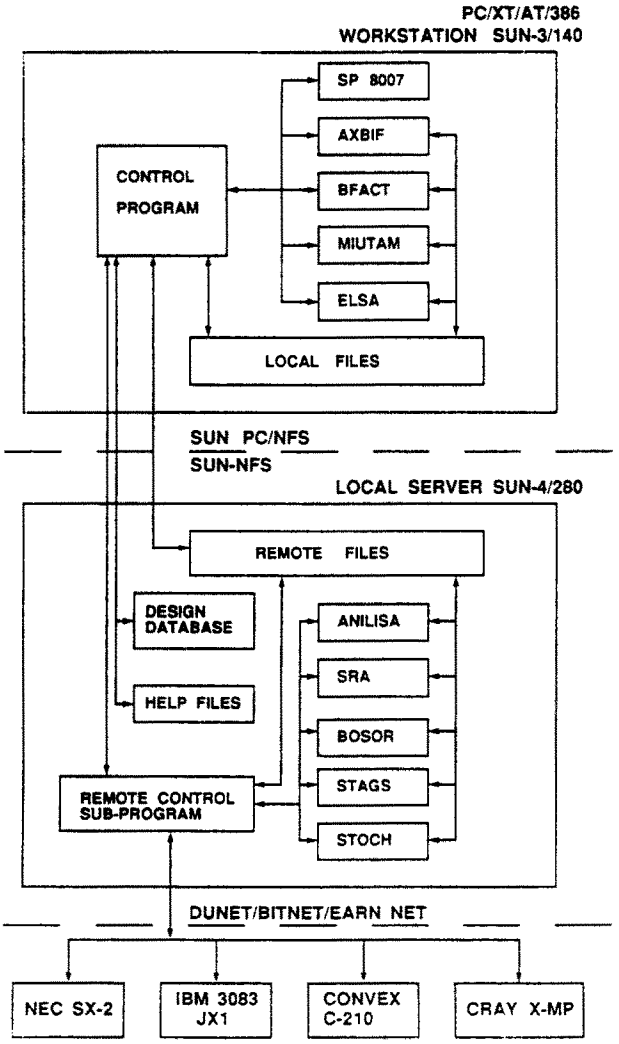

Fig. 5. Schematic layout of the full scale system.

been made operational (Hol, 1989). It has been put together in accordance with a high-level of "Development Standards" (Anonymous, 1984) so that it can serve as a starting base for the full-scale system. Test-site users have been asked to feed back their experience with the pilot system so as to incorporate their findings in the development of the full-scale system.

The final component of DISDECO is defined as an "Expert System" (see Fig. 3). Its purpose is to make available the knowledge and experience of recognized experts. As such its function is parallel to that of the command and control processor, adding intelligence and reasoning capabilities to assist the user. Inclusion of a proven expert system has been opted for. However, acquisition and integration of an expert system requires major efforts for the generation of criteria and specifications. Collection and formalizing of existing knowledge is another major issue requiring a dedicated effort. Thus, whereas the inclusion of an expert system is an essential step to improve the proposed system from a powerful toolbox to a full-fledged assistant, still its implementation will be delayed until the results and experiences with the pilot system have been evaluated.

3. DEVELOPMENT OF "ANILISA"

When DISDECO is finished it will provide an easy access to most of the theoretical knowledge, that has been accumulated by the many scientists who have been active in the field of shell stability, via the advanced interactive and computational facilities offered by the modern high speed 32-bit work stations. Great care is being taken to present the results in a unified form so as to make it easy for the user to proceed step-by-step from the simpler approaches used by the early investigators to the more sophisticated analytical and numerical methods used presently.

This approach is illustrated by the extension of Koiter's b-factor method (Koiter, 1967; Hutchinson and Amazigo, 1967) to anisotropic shells loaded by axial compression, external pressure and torsion.

Anisotropic shell equations

Using the sign convention defined in Fig. 6 the Donnell-type equations for perfect anisotropic shells (Tennyson and Muggeridge, 1969) can be written as

$$L_{A^*}(F) - L_{B^*}(W) = -(1/R)W_{,xx} - (1/2)L_{NL}(W, W) \tag{2}$$

$$L_{B^*}(F) + L_{D^*}(W) = (1/R)F_{,xx} + L_{NL}(F, W) + p \tag{3}$$

where the linear operators are

$$L_{A^*}(\ ) = A^*_{22}(\ )_{,xxxx} - 2A^*_{26}(\ )_{,xxxy} + (2A^*_{12} + A^*_{66})(\ )_{,xxyy} - 2A^*_{16}(\ )_{,xyyy} + A^*_{11}(\ )_{,yyyy} \tag{4}$$

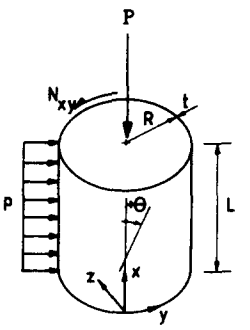

Fig. 6. Notation and sign convention.

$$L_{B^*}(\ ) = B^*_{21}(\ )_{,xxxx} + (2B^*_{26} - B^*_{61})(\ )_{,xxxy} + (B^*_{11} + B^*_{22} - 2B^*_{66})(\ )_{,xxyy} + (2B^*_{16} - B^*_{62})(\ )_{,xyyy} + B^*_{12}(\ )_{,yyyy} \quad (5)$$

$$L_{D^*}(\ ) = D^*_{11}(\ )_{,xxxx} + 4D^*_{16}(\ )_{,xxxy} + 2(D^*_{12} + 2D^*_{66})(\ )_{,xxyy} + 4D^*_{26}(\ )_{,xyyy} + D^*_{22}(\ )_{,yyyy} \quad (6)$$

and the nonlinear operator is

$$L_{NL}(S, T) = S_{,xx}T_{,yy} - 2S_{,xy}T_{,xy} + S_{,yy}T_{,xx}. \quad (7)$$

Commas in the subscripts denote repeated partial differentiation with respect to the independent variables following the comma. The stiffness parameters A^*_{11}, B^*_{11}, D^*_{11}, A^*_{12}, ... etc. are defined in Arbocz and Hol (1989). W is the component of displacement normal to the shell midsurface (here positive inward) and F is the Airy stress function.

Assuming that the eigenvalue problem for the buckling load Λ_c will yield a unique buckling mode $W^{(1)}$ with the associated stress function $F^{(1)}$, a solution, to be valid in the initial post-buckling regime, is sought in the form of the following asymptotic expansions

$$\begin{aligned} \frac{\Lambda}{\Lambda_c} &= 1 + a\xi + b\xi^2 + \cdots \\ W &= W^{(0)} + \xi W^{(1)} + \xi^2 W^{(2)} + \cdots \\ F &= F^{(0)} + \xi F^{(1)} + \xi^2 F^{(2)} + \cdots \end{aligned} \quad (8)$$

where $W^{(1)}$ will be normalized with respect to the shell thickness t and $W^{(2)}$ is orthogonal to $W^{(1)}$ in some appropriate sense.

A formal substitution of this expansion into the nonlinear governing eqns (2) and (3) generates a sequence of equations for the functions appearing in the expansions.

Governing equations of the 0th-order state (pre-buckling problem)

The set of governing equations for $W^{(0)}$ and $F^{(0)}$ are

$$L_{A^*}(F^{(0)}) - L_{B^*}(W^{(0)}) = -(1/R)W^{(0)}_{,xx} - (1/2)L_{NL}(W^{(0)}, W^{(0)}) \quad (9)$$

$$L_{B^*}(F^{(0)}) + L_{D^*}(W^{(0)}) = (1/R)F^{(0)}_{,xx} + L_{NL}(F^{(0)}, W^{(0)}) + p. \quad (10)$$

Since the external loading and the boundary conditions are axisymmetric, therefore the pre-buckling solution will also be axisymmetric. Assuming

$$W^{(0)} = t(W_v + W_p + W_t) + tw_0(x) \quad (11)$$

$$F^{(0)} = (Et^2/cR)[-(1/2)\lambda y^2 - (1/2)\bar{p}x^2 - \bar{\tau}xy + R^2 f_0(x)] \quad (12)$$

then substitution into eqns (9) and (10) and regrouping yields

$$\bar{A}^*_{22} f_0^{iv} - (t/2R)\bar{B}^*_{21} w_0^{iv} = -cw_0'' \quad (13)$$

$$2\bar{B}^*_{21} f_0^{iv} + (t/R)\bar{D}^*_{11} w_0^{iv} = (4cR/t)f_0'' - 4c\lambda w_0'' \quad (14)$$

where $(\ )' = R(\ )_{,x}$, λ is the nondimensional axial load parameter ($\lambda = (cR/Et^2)N_0$), $\bar{p}$ is the nondimensional external pressure ($\bar{p} = (cR^2/Et^2)p$) and $\bar{\tau}$ is the nondimensional torque parameter ($\bar{\tau} = (cR/Et^2)N_{xy}$), positive counter-clockwise. The quantities W_v, W_p and W_t are evaluated by enforcing the circumferential periodicity condition (see Appendix A for details). Equation (13) can be integrated twice yielding

$$f_0'' = (t/2R)(\bar{B}^*_{21}/\bar{A}^*_{22})w_0'' - (c/\bar{A}^*_{22})w_0 + C_1\bar{x} + C_2 \quad (15)$$

where $\bar{x} = x/R$ and the constants of integration C_1 and C_2 are identically equal to zero because of the periodicity condition (see Appendix A for details). Eliminating f_0 between eqns (13) and (14) one obtains

$$(\bar{A}^*_{22}\bar{D}^*_{11} + \bar{B}^{*\,2}_{21})w_0^{iv} + (4cR/t)(\bar{A}^*_{22}\lambda - \bar{B}^*_{21})w_0'' + (4c^2R^2/t^2)w_0 = 0. \tag{16}$$

A fourth-order linear ordinary differential equation with constant coefficients which always admits an exponential solution. Closed form solutions for simply supported and for clamped boundary conditions have been published in the literature (Booton, 1976; Vermeulen, 1982).

Governing equations of the 1st-order state (buckling problem)

The set of governing equations for $W^{(1)}$ and $F^{(1)}$ becomes

$$L_{A^*}(F^{(1)}) - L_{B^*}(W^{(1)}) = -(1/R)W^{(1)}_{,xx} - tw_{0,xx}W^{(1)}_{,yy} \tag{17}$$

$$L_{B^*}(F^{(1)}) + L_{D^*}(W^{(1)}) = (1/R)F^{(1)}_{,xx} + (ERt^2/c)f_{0,xx}W^{(1)}_{,yy} + tw_{0,xx}F^{(1)}_{,yy} - (Et^2/cR)(\lambda W^{(1)}_{,xx} + \bar{p}W^{(1)}_{,yy} - 2\bar{\tau}W^{(1)}_{,xy}). \tag{18}$$

These equations admit separable solutions of the form

$$W^{(1)} = t[w_1(x)\cos n\theta + w_2(x)\sin n\theta] \tag{19}$$

$$F^{(1)} = (ERt^2/c)[f_1(x)\cos n\theta + f_2(x)\sin n\theta] \tag{20}$$

where $\theta = y/R$.

Substitution, regrouping and equating coefficients of like trigonometric terms results in the following system of four linear homogeneous ordinary differential equations with variable coefficients

$$\bar{A}^*_{22}f_1^{iv} - (2\bar{A}^*_{12} + \bar{A}^*_{66})n^2f_1'' + \bar{A}^*_{11}n^4f_1 - 2\bar{A}^*_{26}nf_2''' + 2\bar{A}^*_{16}n^3f_2' - (t/2R)[\bar{B}^*_{21}w_1^{iv} - (\bar{B}^*_{11} + \bar{B}^*_{22} - 2\bar{B}^*_{66})n^2w_1'' + \bar{B}^*_{12}n^4w_1 + (2\bar{B}^*_{26} - \bar{B}^*_{61})nw_2''' - (2\bar{B}^*_{16} - \bar{B}^*_{62})n^3w_2'] + cw_1'' - (ct/R)n^2w_0''w_1 = 0 \tag{21}$$

$$\bar{A}^*_{22}f_2^{iv} - (2\bar{A}^*_{12} + \bar{A}^*_{66})n^2f_2'' + \bar{A}^*_{11}n^4f_2 + 2\bar{A}^*_{26}nf_1''' - 2\bar{A}^*_{16}n^3f_1' - (t/2R)[\bar{B}^*_{21}w_2^{iv} - (\bar{B}^*_{11} + \bar{B}^*_{22} - 2\bar{B}^*_{66})n^2w_2'' + \bar{B}^*_{12}n^4w_2 - (2\bar{B}^*_{26} - \bar{B}^*_{61})nw_1''' + (2\bar{B}^*_{16} - \bar{B}^*_{62})n^3w_1'] + cw_2'' - (ct/R)n^2w_0''w_2 = 0 \tag{22}$$

$$(2R/t)[\bar{B}^*_{21}f_1^{iv} - (\bar{B}^*_{11} + \bar{B}^*_{22} - 2\bar{B}^*_{66})n^2f_1'' + \bar{B}^*_{12}n^4f_1 + (2\bar{B}^*_{26} - \bar{B}^*_{61})nf_2''' - (2\bar{B}^*_{16} - \bar{B}^*_{62})n^3f_2'] + \bar{D}^*_{11}w_1^{iv} - 2(\bar{D}^*_{12} + 2\bar{D}^*_{66})n^2w_1'' + \bar{D}^*_{22}n^4w_1 + 4\bar{D}^*_{16}nw_2''' - 4\bar{D}^*_{26}n^3w_2' - (4cR^2/t^2)f_1'' + (4cR/t)[\lambda w_1'' - \bar{p}n^2w_1 - 2n\bar{\tau}w_2' + n^2(f_0''w_1 + w_0''f_1)] = 0 \tag{23}$$

$$(2R/t)[\bar{B}^*_{21}f_2^{iv} - (\bar{B}^*_{11} + \bar{B}^*_{22} - 2\bar{B}^*_{66})n^2f_2'' + \bar{B}^*_{12}n^4f_2 - (2\bar{B}^*_{26} - \bar{B}^*_{61})nf_1''' + (2\bar{B}^*_{16} - \bar{B}^*_{62})n^3f_1'] + \bar{D}^*_{11}w_2^{iv} - 2(\bar{D}^*_{12} + 2\bar{D}^*_{66})n^2w_2'' + \bar{D}^*_{22}n^4w_2 - 4\bar{D}^*_{16}nw_1''' + 4\bar{D}^*_{26}n^3w_1' - (4cR^2/t^2)f_2'' + (4cR/t)[\lambda w_2'' - \bar{p}n^2w_2 + 2n\bar{\tau}w_1' + n^2(f_0''w_2 + w_0''f_2)] = 0. \tag{24}$$

Further, in order to be able to use the "shooting method" of Keller (1968) to solve the governing equations of the 1st-order state it is necessary, by considering eqns (21) and (23), to eliminate the w_1^{iv} term from eqn (21) and the f_1^{iv} term from eqn (23). Similarly, by considering eqns (22) and (24) one must eliminate the w_2^{iv} term from eqn (22) and the f_2^{iv} term from eqn (24). Finally, some regrouping makes it possible to write the resulting

equations as

$$f_1^{iv} = C_{17}f_1'' - C_{18}f_1 + C_{19}f_2''' + C_{20}f_2' + C_{21}w_1'' + C_{22}w_1 + C_{23}w_2''' + C_{24}w_2' + C_{26}w_0''w_1 + C_{28}\bar{p}w_1 - C_{28}f_0''w_1 + C_{30}\bar{\tau}w_2' - C_{31}\lambda w_1'' - C_{28}w_0''f_1 \quad (25)$$

$$f_2^{iv} = C_{17}f_2'' - C_{18}f_2 - C_{19}f_1''' - C_{20}f_1' + C_{21}w_2'' + C_{22}w_2 - C_{23}w_1''' - C_{24}w_1' + C_{26}w_0''w_2 + C_{28}\bar{p}w_2 - C_{28}f_0''w_2 - C_{30}\bar{\tau}w_1' - C_{31}\lambda w_2'' - C_{28}w_0''f_2 \quad (26)$$

$$w_1^{iv} = C_1f_1'' + C_2f_1 - C_3f_2''' + C_4f_2' + C_5w_1'' - C_6w_1 - C_7w_2''' + C_8w_2' - C_{10}w_0''w_1 + C_{12}\bar{p}w_1 - C_{12}f_0''w_1 + C_{14}\bar{\tau}w_2' - C_{15}\lambda w_1'' - C_{12}w_0''f_1 \quad (27)$$

$$w_2^{iv} = C_1f_2'' + C_2f_2 + C_3f_1''' - C_4f_1' + C_5w_2'' - C_6w_2 + C_7w_1''' - C_8w_1' - C_{10}w_0''w_2 + C_{12}\bar{p}w_2 - C_{12}f_0''w_2 - C_{14}\bar{\tau}w_1' - C_{15}\lambda w_2'' - C_{12}w_0''f_2. \quad (28)$$

The constants $C_1 - C_{31}$ are listed in Arbocz and Hol (1989); f_0'' is given by eqn (15).

This set of homogeneous differential equations with variable coefficients together with the appropriate boundary conditions listed in Arbocz and Hol (1989) form an eigenvalue problem which is solved numerically.

Governing equations of the 2nd-order state (post-buckling problem)

The set of governing equations for $W^{(2)}$ and $F^{(2)}$ is

$$\begin{aligned} L_{A^*}(F^{(2)}) - L_{B^*}(W^{(2)}) = {} & -(1/R)W_{,xx}^{(2)} - tw_{0,xx}W_{,yy}^{(2)} \\ & + (1/2)(t/R)^2n^2\{(w_1w_{1,xx} + w_{1,x}w_{1,x} + w_2w_{2,xx} + w_{2,x}w_{2,x}) \\ & + (w_1w_{1,xx} - w_{1,x}w_{1,x} - w_2w_{2,xx} + w_{2,x}w_{2,x})\cos 2n\theta \\ & + (w_1w_{2,xx} + w_2w_{1,xx} - 2w_{1,x}w_{2,x})\sin 2n\theta\} \end{aligned} \quad (29)$$

$$\begin{aligned} L_{B^*}(F^{(2)}) + L_{D^*}(W^{(2)}) = {} & (1/R)F_{,xx}^{(2)} + (ERt^2/c)f_{0,xx}W_{,yy}^{(2)} + tw_{0,xx}F_{,yy}^{(2)} \\ & - (Et^2/cR)(\lambda W_{,xx}^{(2)} + \bar{p}W_{,yy}^{(2)} - 2\bar{\tau}W_{,xy}^{(2)}) \\ & - (1/2)(Et^3/cR)n^2\{(w_1f_{1,xx} + 2w_{1,x}f_{1,x} + w_{1,xx}f_1 + w_2f_{2,xx} + 2w_{2,x}f_{2,x} + w_{2,xx}f_2) \\ & + [w_1f_{1,xx} - 2w_{1,x}f_{1,x} + w_{1,xx}f_1 - (w_2f_{2,xx} - 2w_{2,x}f_{2,x} + w_{2,xx}f_2)]\cos 2n\theta \\ & + [w_1f_{2,xx} - 2w_{1,x}f_{2,x} + w_{1,xx}f_2 + (w_2f_{1,xx} - 2w_{2,x}f_{1,x} + w_{2,xx}f_1)]\sin 2n\theta\}. \end{aligned} \quad (30)$$

These equations admit separable solutions of the form

$$W^{(2)} = t[w_\alpha(x) + w_\beta(x)\cos 2n\theta + w_\gamma(x)\sin 2n\theta] \quad (31)$$

$$F^{(2)} = (ERt^2/c)[f_\alpha(x) + f_\beta(x)\cos 2n\theta + f_\gamma(x)\sin 2n\theta]. \quad (32)$$

Substituting, regrouping and equating coefficients of like trigonometric terms yields the following system of six linear inhomogeneous ordinary differential equations with variable coefficients

$$\bar{A}_{22}^*f_\alpha^{iv} - (t/2R)\bar{B}_{21}^*w_\alpha^{iv} + cw_\alpha'' = (ct/2R)n^2(w_1w_1'' + w_1'w_1' + w_2w_2'' + w_2'w_2') \quad (33)$$

$$\begin{aligned} & \bar{A}_{22}^*f_\beta^{iv} - (2\bar{A}_{12}^* + \bar{A}_{66}^*)4n^2f_\beta'' + \bar{A}_{11}^*16n^4f_\beta - 4\bar{A}_{26}^*nf_\gamma''' + 16\bar{A}_{16}^*n^3f_\gamma' \\ & \quad - (t/2R)[\bar{B}_{21}^*w_\beta^{iv} - (\bar{B}_{11}^* + \bar{B}_{22}^* - 2\bar{B}_{66}^*)4n^2w_\beta'' + \bar{B}_{12}^*16n^4w_\beta + (2\bar{B}_{26}^* - \bar{B}_{61}^*)2nw_\gamma''' \\ & \quad - (2\bar{B}_{16}^* - \bar{B}_{62}^*)8n^3w_\gamma'] + cw_\beta'' - (4ct/R)n^2w_0''w_\beta = (ct/2R)n^2(w_1w_1'' - w_1'w_1' - w_2w_2'' + w_2'w_2') \end{aligned} \quad (34)$$

$$\bar{A}^*_{22}f^{iv}_\gamma-(2\bar{A}^*_{12}+\bar{A}^*_{66})4n^2f''_\gamma+\bar{A}^*_{11}16n^4f_\gamma+4\bar{A}^*_{26}nf'''_\beta-16\bar{A}^*_{16}n^3f'_\beta$$
$$-(t/2R)[\bar{B}^*_{21}w^{iv}_\gamma-(\bar{B}^*_{11}+\bar{B}^*_{22}-2\bar{B}^*_{66})4n^2w''_\gamma+\bar{B}^*_{12}16n^4w_\gamma-(2\bar{B}^*_{26}-\bar{B}^*_{61})2nw'''_\beta$$
$$+(2\bar{B}_{16}-\bar{B}^*_{62})8n^3w'_\beta]+cw''_\gamma-(4ct/R)n^2w''_0w_\gamma=(ct/2R)n^2(w_1w''_2+w_2w''_1-2w'_1w'_2) \quad (35)$$

$$\bar{B}^*_{21}f^{iv}_\alpha+(t/2R)\bar{D}^*_{11}w^{iv}_\alpha-(2cR/t)f''_\alpha+2c\lambda w''_\alpha$$
$$=-cn^2(w_1f''_1+2w'_1f'_1+w''_1f_1+w_2f''_2+2w'_2f'_2+w''_2f_2) \quad (36)$$

$$\bar{B}^*_{21}f^{iv}_\beta-(\bar{B}^*_{11}+\bar{B}^*_{22}-2\bar{B}^*_{66})4n^2f''_\beta+\bar{B}^*_{12}16n^4f_\beta+(2\bar{B}^*_{26}-\bar{B}^*_{61})2nf'''_\gamma$$
$$-(2\bar{B}^*_{16}-\bar{B}^*_{62})8n^3f'_\gamma+(t/2R)[\bar{D}^*_{11}w^{iv}_\beta-2(\bar{D}^*_{12}+2\bar{D}^*_{66})4n^2w''_\beta+\bar{D}^*_{22}16n^4w_\beta$$
$$+8\bar{D}^*_{16}nw'''_\gamma-32\bar{D}^*_{26}n^3w'_\gamma]-(2cR/t)f''_\beta+2c(\lambda w''_\beta-4n^2\bar{p}w_\beta-4n\bar{\tau}w'_\gamma)$$
$$+8cn^2(w''_0f_\beta+f''_0w_\beta)=-cn^2(w_1f''_1-2w'_1f'_1+w''_1f_1-w_2f''_2+2w'_2f'_2-w''_2f_2) \quad (37)$$

$$\bar{B}^*_{21}f^{iv}_\gamma-(\bar{B}^*_{11}+\bar{B}^*_{22}-2\bar{B}^*_{66})4n^2f''_\gamma+\bar{B}^*_{12}16n^4f_\gamma-(2\bar{B}^*_{26}-\bar{B}^*_{61})2nf'''_\beta$$
$$+(2\bar{B}^*_{16}-\bar{B}^*_{62})8n^3f'_\beta+(t/2R)[\bar{D}^*_{11}w^{iv}_\gamma-2(\bar{D}^*_{12}+2\bar{D}^*_{66})4n^2w''_\gamma+\bar{D}^*_{22}16n^4w_\gamma$$
$$-8\bar{D}^*_{16}nw'''_\beta+32\bar{D}^*_{26}n^3w'_\beta]-(2cR/t)f''_\gamma+2c(\lambda w''_\gamma-4n^2\bar{p}w_\gamma+4n\bar{\tau}w'_\beta)$$
$$+8cn^2(w''_0f_\gamma+f''_0w_\gamma)=-cn^2(w_1f''_2-2w'_1f'_2+w''_1f_2+w_2f''_1-2w'_2f'_1+w''_2f_1). \quad (38)$$

Equation (33) can be integrated twice to yield

$$f''_\alpha=(t/2R)(\bar{B}^*_{21}/\bar{A}^*_{22})w''_\alpha-(c/\bar{A}^*_{22})w_\alpha+(ct/4R)(n^2/\bar{A}^*_{22})(w_1^2+w_2^2)+\tilde{C}_3\bar{x}+\tilde{C}_4 \quad (39)$$

where $\bar{x}=x/R$ and the constants of integration $\tilde{C}_3$ and $\tilde{C}_4$ are identically equal to zero because of the periodicity condition (see Appendix A for details). Eliminating f_α between eqns (33) and (36) one obtains

$$w^{iv}_\alpha=(D_1-D_2\lambda)w''_\alpha-D_3w_\alpha+D_4(w_1^2+w_2^2)-D_5(w_1w''_1+w'_1w'_1+w_2w''_2+w'_2w'_2)$$
$$+D_8(w_1f''_1+2w'_1f'_1+w''_1f_1+w_2f''_2+2w'_2f'_2+w''_2f_2). \quad (40)$$

Further, in order to be able to use the "shooting method" of Keller (1968) to solve the governing equations of the 2nd-order state it is necessary, by considering eqns (34) and (37), to eliminate the w^{iv}_β term from eqn (34) and the f^{iv}_β term from eqn (37). Similarly, by considering eqns (35) and (38) one must eliminate the w^{iv}_γ term from eqn (35) and the f^{iv}_γ term from eqn (38). Finally, some further regrouping makes it possible to write the resulting equations as

$$f^{iv}_\beta=D_9f''_\beta-(D_{10}+D_{17}w''_0)f_\beta+D_{11}f'''_\gamma-D_{12}f'_\gamma-(D_{13}+D_{31}\lambda)w''_\beta-(D_{14}-D_{18}w''_0)w_\beta$$
$$-D_{17}(f''_0-\bar{p})w_\beta-D_{15}w'''_\gamma+(D_{16}+D_{19}\bar{\tau})w'_\gamma+D_{32}(w_1w''_1-w'_1w'_1-w_2w''_2+w'_2w'_2)$$
$$-D_5(w_1f''_1-2w'_1f'_1+w''_1f_1-w_2f''_2+2w'_2f'_2-w''_2f_2) \quad (41)$$

$$f^{iv}_\gamma=D_9f''_\gamma-(D_{10}+D_{17}w''_0)f_\gamma-D_{11}f'''_\beta+D_{12}f'_\beta-(D_{13}+D_{31}\lambda)w''_\gamma$$
$$-(D_{14}-D_{18}w''_0)w_\gamma-D_{17}(f''_0-\bar{p})w_\gamma+D_{15}w'''_\beta-(D_{16}+D_{19}\bar{\tau})w'_\gamma$$
$$+D_{32}(w_1w''_2+w_2w''_1-2w'_1w'_2)-D_5(w_1f''_2-2w'_1f'_2+w''_1f_2+w_2f''_1-2w'_2f'_1+w''_2f_1) \quad (42)$$

$$w^{iv}_\beta=-D_{20}f''_\beta-(D_{21}+D_{22}w''_0)f_\beta+(D_{23}-D_2\lambda)w''_\beta-(D_{24}+D_{17}w''_0)w_\beta-D_{22}(f''_0-\bar{p})w_\beta$$
$$-D_{25}f'''_\gamma+D_{26}f'_\gamma-D_{27}w'''_\gamma+(D_{28}+D_{29}\bar{\tau})w'_\gamma-D_5(w_1w''_1-w'_1w'_1-w_2w''_2+w'_2w'_2)$$
$$-D_8(w_1f''_1-2w'_1f'_1+w''_1f_1-w_2f''_2+2w'_2f'_2-w''_2f_2) \quad (43)$$

$$w_{,}^{iv} = -D_{20}f_{,}''-(D_{21}+D_{22}w_0'')f_{,}+(D_{23}-D_2\lambda)w_{,}''-(D_{24}+D_{17}w_0'')w_{,}$$
$$-D_{22}(f_0''-\bar{p})w_{,}+D_{25}f_{\beta}'''-D_{26}f_{\beta}'+D_{27}w_{\beta}'''-(D_{28}+D_{29}\bar{\tau})w_{\beta}'$$
$$-D_5(w_1w_2''+w_2w_1''-2w_1'w_2')-D_8(w_1f_2''-2w_1'f_2'+w_1''f_2+w_2f_1''-2w_2'f_1'+w_2''f_1). \quad (44)$$

The constants D_1–D_{32} are listed in Arbocz and Hol (1989); f_0'' is given by eqn (15).

This set of inhomogeneous differential equations with variable coefficients together with the appropriate boundary conditions listed in Arbocz and Hol (1989) form a response problem which is solved numerically.

Post-buckling coefficients and imperfection form factors

For perfect shells one is interested in the variation of $\Lambda(\xi)$ with ξ in the vicinity of $\Lambda = \Lambda_c$. Near the bifurcation point Λ_c the asymptotic expansion given in eqn (8) is valid. The post-buckling coefficients "a" and "b" are derived in Arbocz and Hol (1989) yielding

$$a = -(3/2\Lambda_c\hat{\Delta})F^{(1)*}(W^{(1)}, W^{(1)}) \quad (45)$$

$$b = -(1/\Lambda_c\hat{\Delta})[2F^{(1)*}(W^{(1)}, W^{(2)})+F^{(2)*}(W^{(1)}, W^{(1)})+a\Lambda_c\Pi_1+(1/2)(a\Lambda_c)^2\Pi_2] \quad (46)$$

where

$$\hat{\Delta} = 2F^{(1)*}(\dot{W}_c, W^{(1)})+\dot{F}_c^*(W^{(1)}, W^{(1)}) \quad (47)$$

$$\Pi_1 = F^{(1)*}(\dot{W}_c, W^{(2)})+F^{(2)*}(\dot{W}_c, W^{(1)})+\dot{F}_c^*(W^{(1)}, W^{(2)}) \quad (48)$$

$$\Pi_2 = 2F^{(1)*}(\ddot{W}_c, W^{(1)})+\ddot{F}_c^*(W^{(1)}, W^{(1)}) \quad (49)$$

$$(\dot{})_c = \frac{\partial}{\partial\Lambda}(\,)_c. \quad (50)$$

The subscript $(\,)_c$ denotes the fact that the pre-buckling solution is evaluated at the bifurcation point. The shorthand notation used

$$A^*(B, C) = \int\int_S [A_{,xx}B_{,y}C_{,y}+A_{,yy}B_{,x}C_{,x}-A_{,xy}(B_{,x}C_{,y}+B_{,y}C_{,x})]\,dx\,dy \quad (51)$$

was first introduced by Hutchinson and Frauenthal (1969).

For imperfect shells the variation of $\Lambda(\xi, \bar{\xi})$ in the vicinity of the birfurcation point $\Lambda = \Lambda_c$ is given by the following asymptotic expansion (Cohen, 1968) (see also Fig. 7)

$$(\Lambda-\Lambda_c)\xi = a\Lambda_c\xi^2+b\Lambda_c\xi^3+\cdots-\alpha\Lambda_c\bar{\xi}-\beta(\Lambda-\Lambda_c)\bar{\xi}+O(\xi\bar{\xi}). \quad (52)$$

The imperfection form factors "α" and "β" are derived in Arbocz and Hol (1989) yielding

$$\alpha = (1/\Lambda_c\hat{\Delta})[F_c^*(\hat{W}, W^{(1)})+F^{(1)*}(\hat{W}, W_c)] \quad (53)$$

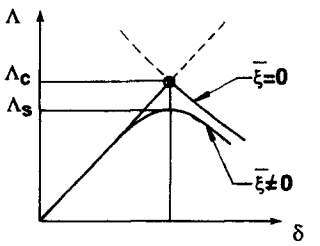

Fig. 7. Equilibrium paths of perfect and imperfect systems.

$$\beta = (1/\hat{\Delta})\{\dot{F}_c^*(\hat{W}, W^{(1)}) + F^{(1)*}(\hat{W}, \dot{W}_c) + \Pi_3 - \alpha\Lambda_c[(1/2)\Pi_4 + \Pi_5]\} \tag{54}$$

where

$$\Pi_3 = \int\int_s \{[A_{11}\dot{W}_{c,x}W^{(1)}_{,x} + A_{12}\dot{W}_{c,y}W^{(1)}_{,y} + A_{16}(\dot{W}_{c,x}W^{(1)}_{,y} + W^{(1)}_{,x}\dot{W}_{c,y})]\hat{W}_{,x}W_{c,x}$$
$$+ [A_{12}\dot{W}_{c,x}W^{(1)}_{,x} + A_{22}\dot{W}_{c,y}W^{(1)}_{,y} + A_{26}(\dot{W}_{c,x}W^{(1)}_{,y} + W^{(1)}_{,x}\dot{W}_{c,y})]\hat{W}_{,y}W_{c,y} + [A_{16}\dot{W}_{c,x}W^{(1)}_{,x}$$
$$+ A_{26}\dot{W}_{c,y}W^{(1)}_{,y} + A_{66}(\dot{W}_{c,x}W^{(1)}_{,y} + W^{(1)}_{,x}\dot{W}_{c,y})](\hat{W}_{,x}W_{c,y} + W_{c,x}\hat{W}_{,y})\}\,\mathrm{d}x\,\mathrm{d}y \tag{55}$$

$$\Pi_4 = 2F^{(1)*}(\ddot{W}_c, W^{(1)}) + \ddot{F}_c^*(W^{(1)}, W^{(1)}) \tag{56}$$

$$\Pi_5 = \int\int_s \{[A_{11}\dot{W}_{c,x}W^{(1)}_{,x} + A_{12}\dot{W}_{c,y}W^{(1)}_{,y} + A_{16}(\dot{W}_{c,x}W^{(1)}_{,y} + W^{(1)}_{,x}\dot{W}_{c,y})]\dot{W}_{c,x}W^{(1)}_{,x}$$
$$+ [A_{12}\dot{W}_{c,x}W^{(1)}_{,x} + A_{22}\dot{W}_{c,y}W^{(1)}_{,y} + A_{26}(\dot{W}_{c,x}W^{(1)}_{,y} + W^{(1)}_{,x}\dot{W}_{c,y})]\dot{W}_{c,y}W^{(1)}_{,y} + [A_{16}\dot{W}_{c,x}W^{(1)}_{,x}$$
$$+ A_{26}\dot{W}_{c,y}W^{(1)}_{,y} + A_{66}(\dot{W}_{c,x}W^{(1)}_{,y} + W^{(1)}_{,x}\dot{W}_{c,y})](\dot{W}_{c,x}W^{(1)}_{,y} + W^{(1)}_{,x}\dot{W}_{c,y})\}\,\mathrm{d}x\,\mathrm{d}y. \tag{57}$$

Since the initial imperfection is assumed to be

$$\bar{W} = \bar{\xi}\hat{W}. \tag{58}$$

$\hat{W}$ represents the shape of the initial imperfection. Notice that if the initial imperfection is assumed to be affine to the buckling mode, then $\hat{W} = W^{(1)}$.

As can be seen from Fig. 7 the buckling load of the imperfect structure Λ_s occurs at the "limit point" of the pre-buckling states. If the limit point is close enough to the bifurcation point then Λ_s, the maximum load that the structure can support prior to buckling, can also be evaluated from eqn (52) by maximizing Λ with respect to ξ. For the many practical applications where a unique buckling mode is associated with the lowest buckling load and the buckling and initial post-buckling behaviour are symmetric with respect to the buckling displacement, the first post-buckling coefficient "a" is identically equal to zero. In this case using eqn (52) to maximize Λ with respect to ξ leads to the Modified Koiter Formula (Cohen, 1971)

$$(1-\rho_s)^{3/2} = (3/2)\sqrt{-3\alpha^2 b}[1-(\beta/\alpha)(1-\rho_s)]|\bar{\xi}| \tag{59}$$

where $\rho_s = \Lambda_s/\Lambda_c$ and $\bar{\xi}$ is the normalized amplitude of the initial imperfection. It should be emphasized that in all cases presented, $\bar{\xi}$ has been normalized with respect to the shell thickness t and not some effective thickness of the stiffener-shell combination.

Generalized "load-shortening" relation

Information concerning the extent to which buckling can be expected to be gradual or sudden can be obtained from the post-buckling variation of the applied variable load Λ with the generalized displacement Δ. Notice that $\Lambda \cdot \Delta$ represents the decrease in potential energy of the applied variable loads. Thus

$$\Lambda \cdot \Delta = \int\int_s \bar{N}_{\alpha\beta}\varepsilon_{\alpha\beta}\,\mathrm{d}x\,\mathrm{d}y \tag{60}$$

where $\bar{N}_{\alpha\beta}$ is the variable applied stress resultant and $\varepsilon_{\alpha\beta}$ is the corresponding linear strain. Notice that $\varepsilon_{\alpha\beta}$ can be obtained from the nonlinear strain-displacement relations

$$E_{\alpha\beta} = \varepsilon_{\alpha\beta} + \tfrac{1}{2}W_{,\alpha}W_{,\beta}. \tag{61}$$

Using the perturbation expansions defined by eqn (8) one gets upon substitution and regrouping

$$\Lambda\cdot\Delta=\int\int_s \bar{N}_{\alpha\beta}[E^{(0)}_{\alpha\beta}-(1/2)W^{(0)}_{,\alpha}W^{(0)}_{,\beta}]\,dx\,dy$$
$$+\xi\left\{\int\int_s \bar{N}_{\alpha\beta}[E^{(1)}_{\alpha\beta}-(1/2)(W^{(1)}_{,\alpha}W^{(0)}_{,\beta}+W^{(0)}_{,\alpha}W^{(1)}_{,\beta})]\,dx\,dy\right\}$$
$$+\xi^2\left\{\int\int_s \bar{N}_{\alpha\beta}[E^{(2)}_{\alpha\beta}-(1/2)(W^{(2)}_{,\alpha}W^{(0)}_{,\beta}+W^{(0)}_{,\alpha}W^{(2)}_{,\beta})-(1/2)W^{(1)}_{,\alpha}W^{(1)}_{,\beta}]\,dx\,dy\right\}+\cdots. \quad (62)$$

Since the applied external load and the pre-buckling state is axisymmetric, therefore for an asymmetric buckling mode

$$\int\int_s \bar{N}_{\alpha\beta}[E^{(1)}_{\alpha\beta}-(1/2)(W^{(1)}_{,\alpha}W^{(0)}_{,\beta}+W^{(0)}_{,\alpha}W^{(1)}_{,\beta})]\,dx\,dy=0. \quad (63)$$

Using Taylor series expansions at $\Lambda=\Lambda_c$ for the pre-buckling quantities in eqn (62) and specializing the results to the cases where the first post-buckling coefficient "a" is identically equal to zero, one obtains after some regrouping

$$\Lambda\cdot\Delta=\Lambda\cdot\Delta_c+(\Lambda-\Lambda_c)\left\{\int\int_s \bar{N}_{\alpha\beta}[\dot{E}_{\alpha\beta_c}-(1/2)(W_{c,\alpha}\dot{W}_{c,\beta}+\dot{W}_{c,\alpha}W_{c,\beta})]\,dx\,dy\right.$$
$$\left.+(1/b\Lambda_c)\int\int_s \bar{N}_{\alpha\beta}[E^{(2)}_{\alpha\beta}-(1/2)(W^{(2)}_{,\alpha}W_{c,\beta}+W_{c,\alpha}W^{(2)}_{,\beta})-(1/2)W^{(1)}_{,\alpha}W^{(1)}_{,\beta}]\,dx\,dy\right\}+\cdots \quad (64)$$

where

$$\Lambda\cdot\Delta_c=\int\int_s \bar{N}_{\alpha\beta}[E_{\alpha\beta_c}-(1/2)W_{c,\alpha}W_{c,\beta}]\,dx\,dy \quad (65)$$

$$E_{\alpha\beta_c}=E^{(0)}_{\alpha\beta}\Big|_{\Lambda=\Lambda_c}, \quad (66)$$

$$(\dot{})_c=\frac{\partial}{\partial\Lambda}(\,)_c. \quad (67)$$

Notice that if "a" is identically equal to zero then from eqn (8)

$$\xi^2=(1/b\Lambda_c)(\Lambda-\Lambda_c). \quad (68)$$

Finally, the generalized displacement Δ can be written as

$$\Delta=\Delta_c+(\rho-1)\left\{\int\int_s (\bar{N}_{\alpha\beta}/\Lambda)[\dot{E}_{\alpha\beta_c}-(1/2)(W_{c,\alpha}\dot{W}_{c,\beta}+\dot{W}_{c,\alpha}W_{c,\beta})]\,dx\,dy\right.$$
$$\left.+(1/b)\int\int_s (\bar{N}_{\alpha\beta}/\Lambda)[E^{(2)}_{\alpha\beta}-(1/2)(W^{(2)}_{,\alpha}W_{c,\beta}+W_{c,\alpha}W^{(2)}_{c,\beta})-(1/2)W^{(1)}_{,\alpha}W^{(1)}_{,\beta}]\,dx\,dy\right\}+\cdots \quad (69)$$

where now $\rho=\Lambda/\Lambda_c$, $(\dot{})=\partial(\,)/\partial\rho$ and $\Delta_c=$ generalized displacement just before buckling.

Computing the slope of the variable load vs generalized displacement curve just before buckling one obtains

$$K_c = \frac{\partial \Lambda}{\partial \Delta_c}\bigg]_{\Lambda=\Lambda_c} = \left\{\frac{\partial \Delta_c}{\partial \Lambda}\bigg]_{\Lambda=\Lambda_c}\right\}^{-1}$$

$$= \left\{\int\int_S (\bar{N}_{\alpha\beta}/\Lambda)[\dot{E}_{\alpha\beta_c} - (1/2)(W_{c,\alpha}\dot{W}_{c,\beta} + \dot{W}_{c,\alpha}W_{c,\beta})]\,dx\,dy\right\}^{-1}. \tag{70}$$

Conversely, the slope of the variable load vs generalized displacement curve just after buckling is given by

$$K_c^* = \frac{\partial \Lambda}{\partial \Delta}\bigg]_{\Lambda=\Lambda_c} = \left\{\frac{\partial \Delta}{\partial \Lambda}\bigg]_{\Lambda=\Lambda_c}\right\}^{-1}$$

$$= \left\{\int\int_S (\bar{N}_{\alpha\beta_c}/\Lambda)[\dot{E}_{\alpha\beta_c} - (1/2)(W_{c,\alpha}\dot{W}_{c,\beta} + \dot{W}_{c,\alpha}W_{c,\beta})]\,dx\,dy\right.$$

$$\left. + (1/b)\int\int_S (\bar{N}_{\alpha\beta}/\Lambda)[E^{(2)}_{\alpha\beta} - (1/2)(W^{(2)}_{,\alpha}W_{c,\beta} + W_{c,\alpha}W^{(2)}_{,\beta}) - (1/2)W^{(1)}_{,\alpha}W^{(1)}_{,\beta}]\,dx\,dy\right\}^{-1}. \tag{71}$$

As can be seen from Fig. 8, the angle of the initial slope just after buckling, $\tilde{\theta}^*$, where

$$\tilde{\theta}^* = \tan^{-1}(\varepsilon_M K_c^*) \tag{72}$$

is indeed helpful in determining whether the buckling will be gradual or catastrophic. Notice that it is customary to normalize the generalized displacement Δ by the appropriate membrane strain ε_M (the strain which corresponds to the applied variable load) so that for membrane pre-buckling the angle of the fundamental path $\tilde{\theta} = \tan^{-1}(\varepsilon_M K_c) = 45°$.

4. NUMERICAL ANALYSIS

Introducing as a unified variable the 16-dimensional vector $\mathbf{Y}^{(1)}$ defined as follows

$$Y^{(1)}_1 = f_1, \quad Y^{(1)}_2 = f_2, \quad Y^{(1)}_3 = w_1, \quad Y^{(1)}_4 = w_2, \quad Y^{(1)}_5 = f'_1, \ldots, Y^{(1)}_{16} = w'''_2 \tag{73}$$

then the system of eqns (21)–(24) can be reduced to the following (nonlinear) eigenvalue problem

$$\frac{d}{d\bar{x}}\mathbf{Y}^{(1)} = \mathbf{f}^{(1)}(\bar{x}, \mathbf{Y}^{(0)}, \mathbf{Y}^{(1)}; \lambda, \bar{p}, \bar{\tau}) \tag{74}$$

$$\bar{\bar{B}}^{(1)}_1\mathbf{Y}^{(1)}(\bar{x}=0) + \bar{\bar{B}}^{(1)}_2\mathbf{Y}^{(1)}(\bar{x}=L/R) = 0 \tag{75}$$

where the components of the 8×16 matrices $\bar{\bar{B}}^{(1)}_1$ and $\bar{\bar{B}}^{(1)}_2$ depend on the boundary con-

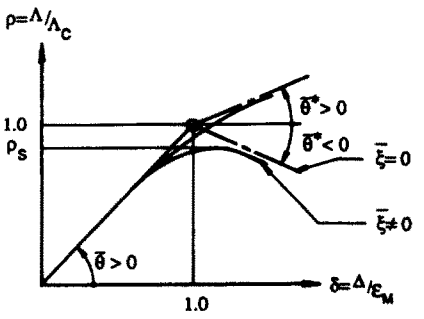

Fig. 8. Generalized "load-shortening" curves.

ditions at the shell edges. Notice that the four-dimensional vector

$$\mathbf{Y}^{(0)} = [w_0, w_0', w_0'', w_0''']^{\mathrm{T}} \tag{76}$$

contains the known solution of eqn (16), the pre-buckling problem.

Introducing further, as another unified variable, the 20-dimensional vector $\mathbf{Y}^{(2)}$ defined as follows

$$Y_1^{(2)} = f_\beta, \quad Y_2^{(2)} = f_{\beta\beta}, \quad Y_3^{(2)} = w_\alpha, \quad Y_4^{(2)} = w_\beta, \quad Y_5^{(2)} = w_{\beta\beta}, \quad Y_6^{(2)} = f_\beta', \ldots, Y_{20}^{(2)} = w_{\beta\beta}''' \tag{77}$$

then the system of eqns (40)–(44) can be reduced to the following inhomogeneous two-point boundary value problem

$$\frac{\mathrm{d}}{\mathrm{d}\bar{x}}\mathbf{Y}^{(2)} = \mathbf{f}^{(2)}(\bar{x}, \mathbf{Y}^{(0)}, \mathbf{Y}^{(2)}; \lambda, \bar{p}, \bar{\tau}) + \hat{\mathbf{f}}(\bar{x}, \mathbf{Y}^{(1)}) \tag{78}$$

$$\bar{\bar{B}}_1^{(2)}\mathbf{Y}^{(2)}(\bar{x} = 0) + \bar{\bar{B}}_2^{(2)}\mathbf{Y}^{(2)}(\bar{x} = L/R) = 0 \tag{79}$$

where once again the components of the 10×20 boundary matrices $\bar{\bar{B}}_1^{(2)}$ and $\bar{\bar{B}}_2^{(2)}$ depend on the boundary conditions at the shell edges. Notice that here the four-dimensional vector $\mathbf{Y}^{(0)}$ contains the known solution of the pre-buckling problem [eqn (16)] and that the 16-dimensional vector $\mathbf{Y}^{(1)}$ is the eigenvector of the buckling problem [eqns (74–75)].

Because of earlier successful experiences with the method (Arbocz and Sechler, 1974; Liu, 1988), it was decided to solve both the buckling problem [eqns (74–75)] and the post-buckling problem [eqns (78–79)] by the numerical technique known as "parallel shooting over n-intervals" (Keller, 1968).

Solution of the buckling problem

To solve the buckling problem a generalization of Stodola's method (Von Kármán and Biot, 1940) for the calculation of the asymmetric buckling loads and the corresponding buckling modes of circular cylindrical shells is used. This generalization was first published by Cohen (1968).

The applied loading consists of axial compression, internal or external pressure and clockwise or counter-clockwise torque. It is assumed to have a uniform spatial distribution and is divided into a fixed part and a variable part. The magnitude of the variable part is allowed to vary in proportion to a load parameter Λ. This leads to an eigenvalue problem for the critical load Λ_c. In eqn (74) the user can select Λ_c to be the critical value of either the normalized axial load λ, or the normalized external pressure $\bar{p}$ or the normalized torque $\bar{\tau}$.

Because of the nonlinear dependence of the pre-buckling state on the variable load Λ, in general it is necessary to approach the critical eigenvalue (for a given circumferential wave number n) by the solution of a sequence of modified (linearized) eigenvalue problems. The equations are obtained by restricting the search for eigenvalues to a sufficiently small neighbourhood of an estimate $\Lambda = \Lambda_e$ so that in this neighbourhood the functions $\mathbf{Y}^{(0)}$ have a linear dependence on Λ. Setting

$$\Lambda = \Lambda_e + \mu \tag{80}$$

one has to first order in μ

$$\mathbf{Y}^{(0)}(\Lambda) = \mathbf{Y}^{(0)}(\Lambda_e) + \mu\dot{\mathbf{Y}}^{(0)}(\Lambda_e) \tag{81}$$

where

$$\dot{\mathbf{Y}}^{(0)} = \frac{\partial}{\partial\Lambda}\mathbf{Y}^{(0)}.$$

Substituting this expression into eqns (74)–(75) and using λ as the variable load yields the following modified (linearized) eigenvalue problem

$$\frac{\mathrm{d}}{\mathrm{d}\bar{x}}\mathbf{Y}^{(1)} = \mathbf{f}^{(1)}(\bar{x}, \mathbf{Y}^{(0)}, \mathbf{Y}^{(1)}; \Lambda_e, \bar{p}, \bar{\tau}) + \mu g^{(1)}(\bar{x}, \dot{\mathbf{Y}}^{(0)}, \mathbf{Y}^{(1)}) \tag{82}$$

$$\bar{\bar{B}}_1^{(1)}\mathbf{Y}^{(1)}(\bar{x}=0) + \bar{\bar{B}}_2^{(1)}\mathbf{Y}^{(1)}(\bar{x}=L/R) = 0. \tag{75}$$

Notice that each of the "effective load terms" is split into a part independent of μ and a second part linear in μ. The iteration equations are obtained by setting $\mu = 1$ in the second parts of the "effective load terms" and interpreting the buckling mode variables of these parts as being known inputs from the previous iteration. Thus the first parts of the "effective load terms" become homogeneous terms and the second parts become inhomogeneous terms for the equivalent linearized problem of each iteration. Thus one must solve repeatedly

$$\frac{\mathrm{d}}{\mathrm{d}\bar{x}}\mathbf{Y}^{(k)} = \mathbf{f}^{(1)}(\bar{x}, \mathbf{Y}^{(0)}, \mathbf{Y}^{(k)}; \Lambda_e, \bar{p}, \bar{\tau}) + g^{(1)}(\bar{x}, \dot{\mathbf{Y}}^{(0)}, \mathbf{Y}^{(k-1)}) \tag{83}$$

$$\bar{\bar{B}}_1^{(1)}\mathbf{Y}^{(k)}(\bar{x}=0) + \bar{\bar{B}}_2^{(1)}\mathbf{Y}^{(k)}(\bar{x}=L/R) = 0 \tag{84}$$

where

$\mathbf{Y}^{(k)}$ = buckling mode of the kth iteration

$\mathbf{Y}^{(k-1)}$ = buckling mode of the $(k-1)$th iteration.

After each iteration the corresponding eigenvalue estimate $\mu^{(k)}$ is calculated by evaluating the following Rayleigh quotient

$$\mu^{(k)} = (\sigma^{(k)}, u^{(k)}; \sigma^{(k-1)}, u^{(k-1)})/(\sigma^{(k)}, u^{(k)}; \sigma^{(k)}, u^{(k)}) \tag{85}$$

where the inner products are defined as follows

$$\begin{aligned}
&(\sigma^{(k)}, u^{(k)}; \sigma^{(k-1)}, u^{(k-1)}) \\
&= \int\int_S [\dot{N}_x^{(0)} W_{,x}^{(k)} W_{,x}^{(k-1)} + \dot{N}_y^{(0)} W_{,y}^{(k)} W_{,y}^{(k-1)} + \dot{N}_{xy}^{(0)}(W_{,x}^{(k)} W_{,y}^{(k-1)} + W_{,x}^{(k-1)} W_{,y}^{(k)})]\,\mathrm{d}x\,\mathrm{d}y \\
&\quad + \int\int_S [N_x^{(k)} \dot{W}_{,x}^{(0)} W_{,x}^{(k-1)} + N_y^{(k)} \dot{W}_{,y}^{(0)} W_{,y}^{(k-1)} + N_{xy}^{(k)}(\dot{W}_{,x}^{(0)} W_{,y}^{(k-1)} + W_{,x}^{(k-1)} \dot{W}_{,y}^{(0)})]\,\mathrm{d}x\,\mathrm{d}y \\
&\quad + \int\int_S [N_x^{(k-1)} \dot{W}_{,x}^{(0)} W_{,x}^{(k)} + N_y^{(k-1)} \dot{W}_{,y}^{(0)} W_{,y}^{(k)} + N_{xy}^{(k-1)}(\dot{W}_{,x}^{(0)} W_{,y}^{(k)} + W_{,x}^{(k)} \dot{W}_{,y}^{(0)})]\,\mathrm{d}x\,\mathrm{d}y.
\end{aligned} \tag{86}$$

The iterations are continued until the sum $\Lambda_e^{(k)} + \mu^{(k)}$ remains essentially constant at the value Λ_1. A suitable choice for the sequence $\Lambda_e^{(k)}$ is $\Lambda_e^{(1)} = 0$ and $\Lambda_e^{(k)} = \Lambda_e^{(k-1)} + (1/2)\mu^{(k-1)}$ for $k > 1$, where the "relaxation factor" 1/2 is inserted in order to assure that at each stage $\Lambda_e^{(k)} < \Lambda_1$. Cohen (1968) has shown that in order to insure that the eigenvalues $\mu^{(k)}$ are real it is necessary that $\Lambda_e^{(k)} < \Lambda_1$. For further details of the solution procedure the interested reader should consult Arbocz and Hol (1989) and Cohen (1968).

Solution of the post-buckling problem

Once the pre-buckling solution vector $\mathbf{Y}^{(0)}$ and the solution of the buckling problem, the eigenvalue Λ_c and the corresponding eigenvector $\mathbf{Y}^{(1)}$ are known, the post-buckling problem is governed by

$$\frac{\mathrm{d}}{\mathrm{d}\bar{x}}\mathbf{Y}^{(2)} = \mathbf{f}^{(2)}(\bar{x}, \mathbf{Y}^{(0)}, \mathbf{Y}^{(2)}; \Lambda_c, \bar{p}, \bar{\tau}) + \hat{\mathbf{f}}(\bar{x}, \mathbf{Y}^{(1)}) \tag{87}$$

$$\bar{\bar{B}}_1^{(2)}\mathbf{Y}^{(2)}(\bar{x}=0) + \bar{\bar{B}}_2^{(2)}\mathbf{Y}^{(2)}(\bar{x}=L/R) = 0. \tag{88}$$

Due to the often complicated functions of x represented by the known solution vectors $\mathbf{Y}^{(0)}$ and $\mathbf{Y}^{(1)}$ anything but a numerical solution of this linear, inhomogeneous two-point boundary value problem is out of the question. A detailed description of the method used is given in Keller (1968) and Arbocz and Hol (1989). Parallel shooting over n-intervals is slower than a coarse standard finite difference or finite element scheme. However, if the length of the intervals of integration is chosen properly so that numerical instabilities are avoided, then this method gives more accurate results. Also, since the step size is changed automatically so as to satisfy the chosen convergence criterion, a single run is sufficient to obtain a converged solution. Thus it is not necessary to repeat the solution with different step sizes to ascertain that a properly converged solution has been found, as is the recommended practice with the standard finite difference or finite element codes.

It is well known that for the linearized two-point boundary value problem in principle Newton's method yields the correct initial value $\mathbf{S}^{(2)}$ directly without the need of iterations (Keller, 1968). In later work it was found that the numerical accuracy of the solution can be improved greatly by a few iterations, whereby the Jacobian is kept constant and only the right-hand side is varied (Arbocz and Hol, 1989). The solution of the associated initial value problems and the corresponding variational equations is done by the library subroutine DEQ from Caltech's Willis Booth Computer Center. DEQ uses the method of Runge–Kutta–Gill to compute starting values for an Adams–Moulton predictor–corrector scheme. As mentioned earlier, the program includes an option with variable interval size and it uses automatic truncation error control. For shells with an $L/R = 1.0$, parallel shooting over eight intervals is used. This actually involves the numerical integration of six 440-dimensional and two 220-dimensional vector equations. These high dimensions are due to the simultaneous integration of the variational equations and the corresponding initial value problem.

Finally, after the solution of the post-buckling problem has been obtained, one must evaluate the integrals involved in the definition of the post-buckling coefficients "a" and "b" [eqns (45–49)], of the imperfection form factors "α" and "β" [eqns (53–57)], of the angle of the fundamental path $\tilde{\theta}$ and of the angle of the initial slope just after buckling $\tilde{\theta}^*$ [eqns (70–71)]. It has been shown in Arbocz and Sechler (1976) that it is advantageous to evaluate the above integrals by solving initial value problems rather than using numerical integration schemes. This same approach is used here. The interested reader should consult Arbocz and Hol (1989) for further details.

5. NUMERICAL RESULTS

Thanks to the extensive NASA sponsored research programs carried out in the sixties and the early seventies it is known that the degree of imperfection sensitivity of thin-walled shell structures depends on the combination of shell geometry and the type of the applied loading. The use of Koiter's general elastic post-buckling theory has been widely explored and it was also found that boundary conditions (Hutchinson and Frauenthal, 1969) and nonlinear modal interactions (Byskov and Hutchinson, 1977) can have a profound effect on the imperfection sensitivity predictions. Furthermore it has been shown by Hutchinson and Frauenthal (1969) for orthotropic cylinders, and by Tennyson *et al.* (1978) for anisotropic shells, that for reliable prediction of the post-buckling behaviour one must use a rigorous pre-buckling analysis.

Thus, although the computational module ANILISA has the capability of using a membrane pre-buckling analysis, in this paper only results of the rigorous pre-buckling branch are included. To test the accuracy and reliability of ANILISA among others the following published results have been partially reproduced:

1. Hutchinson and Frauenthal's (1969) work on the post-buckling behaviour of stiffened cylindrical shells;
2. Tennyson *et al.*'s (1978) work on the buckling of imperfect anisotropic cylinders under combined loading.

As can be seen from Tables 1 and 2 the agreement is good, for the anisotropic shell

Table 1. Comparison of results using Hutchinson's orthotropic shell $A_s/d_sE = 1.0$, $EI_s/d_sD = 100$, $e_s/t = -6.0$ (outside), $GJ/d_sD = 0$

SS-3 Boundary condition ($N_x = -N_0$, $v = W = 0$, $M_x = 0$)

		n	nL/R	λ_c	b	$\bar{b}$	θ_c	θ_c^*
$Z = 300$	(Hutchinson and Frauenthal, 1969)		6.5	8.79	−0.012	−0.0042	36.0	−142.0
	ANILISA	8	6.24	8.813	−0.0119	−0.00379	28.1	−149.8
$Z = 500$	(Hutchinson and Frauenthal, 1969)		10.6	5.04	−0.029	−0.0130	43.0	−136.0
	ANILISA	11	11.08	5.046	−0.0270	−0.0113	37.5	−141.0
$Z = 750$	(Hutchinson and Frauenthal, 1969)		13.1	3.75	−0.034	−0.0210	44.0	−135.0
	ANILISA	11	13.57	3.752	−0.0333	−0.0204	40.1	−138.9
$Z = 1000$	(Hutchinson and Frauenthal, 1969)		14.3	3.25	−0.030	−0.0230	45.0	−135.0
	ANILISA	10	14.24	3.243	−0.0306	−0.0233	41.0	−138.0

C-4 Boundary condition ($u = v = W = W_{,x} = 0$)

		n	nL/R	λ_c	b	$\bar{b}$	θ_c	θ_c^*
$Z = 500$	(Hutchinson and Frauenthal, 1969)		10.45	10.44	−0.056	−0.064	45.0	−135.0
	ANILISA	10	10.07	10.480	−0.0526	−0.0540	44.8	−134.9
$Z = 1000$	(Hutchinson and Frauenthal, 1969)		17.0	6.07	−0.046	−0.040	45.0	−135.0
	ANILISA	12	17.09	6.076	−0.0459	−0.0384	45.0	−134.5

Note: $\bar{b} = \alpha^2 b$; θ_c and θ_c^* are given in degrees.

Table 2. Comparison of results using Booton's anisotropic shell (30°, 0°, −30°), $R/t = 100$, $\bar{Z} = L^2/Rt = 200$, $t = 0.0267$

C-4 Boundary condition ($u = v = W = W_{,x} = 0$)

	n	Booton (1976)	ANILISA	Units
Axial compression	6	−6785.0	−6780.1	lbs
External pressure	9	27.34	27.348	psi
Clockwise torsion	9	7523.0	7522.3	in lb
Counter-clockwise torsion	9	8228.0	8229.3	in lb

even very good. The differences in the orthotropic shell results are due to the fact that Hutchinson and Frauenthal (1969) treat nL/R as a continuous variable, whereas for ANILISA the length over radius is specified and n is treated as an integer during the search for the lowest eigenvalue.

To illustrate the capabilities of ANILISA one of the glass/epoxy (30°, 0°, −30°) composite cylindrical shells tested by Booton (1976) is used. Its geometric and material data are given in Table 3. In the following, the initial imperfection sensitivity computations are based on the assumption that the shapes of the initial imperfections are affine to the corresponding buckling modes. Thus

$$\bar{W} = \bar{\xi}\hat{W} = \bar{\xi}t(w_1 \cos n\theta + w_2 \sin n\theta). \tag{89}$$

Also in all cases only the imperfection sensitivity of the lowest buckling load is calculated.

Axial compression

The normalized buckling load λ_c and the second imperfection sensitivity coefficient $\bar{b} = \alpha^2 b$ are plotted in Fig. 9 as a function of the modified Batdorf parameter $\bar{Z} = L^2/Rt$ for simply supported ($N_x = -N_0$, $v = W = 0$, $M_x = 0$) anisotropic shells. At the lower part of the figure the circumferential wave numbers n at which the lowest buckling loads occur are

Table 3. Booton's anisotropic shell (30°, 0°, −30°). $R/t = 100$, $\bar{Z} = L^2/Rt = 200$, $t = 0.0267$

$$\begin{bmatrix} \varepsilon_x \\ \varepsilon_y \\ \gamma_{xy} \end{bmatrix} = \frac{1}{Et}\begin{bmatrix} 1.3751 & -0.7582 & 0 \\ -0.7582 & 2.6292 & 0 \\ 0 & 0 & 4.8885 \end{bmatrix}\begin{bmatrix} N_x \\ N_y \\ N_{xy} \end{bmatrix} + \frac{t}{2c}\begin{bmatrix} 0 & 0 & 0.1785 \\ 0 & 0 & -0.0096 \\ 0.7430 & 0.1965 & 0 \end{bmatrix}\begin{bmatrix} \kappa_x \\ \kappa_y \\ \kappa_{xy} \end{bmatrix}$$

$$\begin{bmatrix} M_x \\ M_y \\ \frac{M_{xy}+M_{yx}}{2} \end{bmatrix} = \frac{t}{2c}\begin{bmatrix} 0 & 0 & -0.7430 \\ 0 & 0 & -0.1965 \\ -0.1785 & 0.0096 & 0 \end{bmatrix}\begin{bmatrix} N_x \\ N_y \\ N_{xy} \end{bmatrix} + D\begin{bmatrix} 0.5634 & 0.2214 & 0 \\ 0.2214 & 0.3898 & 0 \\ 0 & 0 & 0.1856 \end{bmatrix}\begin{bmatrix} \kappa_x \\ \kappa_y \\ \kappa_{xy} \end{bmatrix}$$

where $c = \sqrt{3(1-\nu^2)}$, $D = Et^3/4c^2$ and $E = 5.83 \times 10^6$ psi, $\nu = 0.363$.

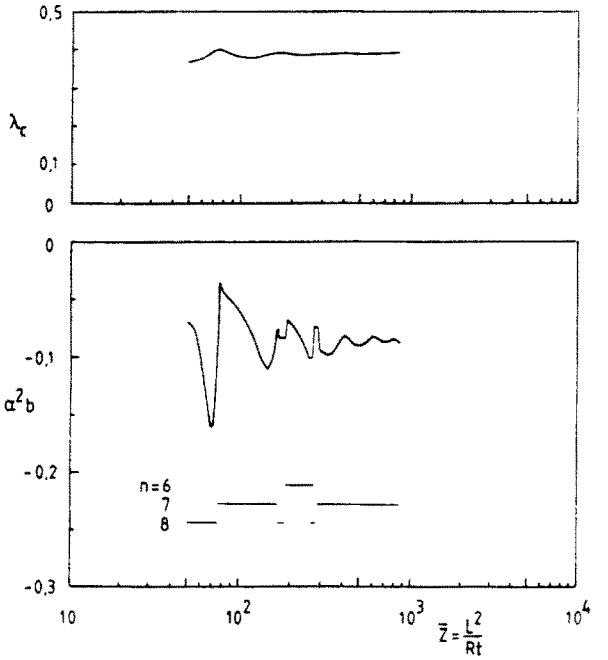

Fig. 9. Perfect shell buckling loads and imperfection sensitivity coefficients for simply supported anisotropic shells under axial compression.

indicated. Notice that sharp changes in the second imperfection sensitivity coefficient $\bar{b} = \alpha^2 b$ always occur at places where there is a change in the critical circumferential wave number n. In Fig. 10 the pre-buckling, buckling and post-buckling mode shapes of a relatively short shell ($\bar{Z} = 50$) and of a shell of moderate length ($\bar{Z} = 400$) are displayed. The amplitudes of the buckling modes are normalized by the wall thickness t, and as has been proven by Booton (1976), one of the components (here w_1) is symmetric and the other antisymmetric with respect to the mid-plane of the shell in the axial direction. Notice that for better illustration all three post-buckling modes are plotted normalized to one using as divisor their maximum amplitudes indicated in the figure. Also, the axial distances $\bar{x} = 0.354$ and $\bar{x} = 1.0$ are the midlengths of shells yielding the (L/R) values that correspond to $\bar{Z} = 50$ and $\bar{Z} = 400$, respectively.

To investigate the effect of different boundary conditions in Fig. 11 the normalized buckling load λ_c and the second imperfection sensitivity coefficient $\bar{b} = \alpha^2 b$ are shown for fully clamped ($u = v = W = W_{,x} = 0$) anisotropic shells. At low $\bar{Z}$ values the sharp changes in $\bar{b} = \alpha^2 b$ occur at either the locations where there is a jump in the critical circumferential wave number n, or as has been shown in Arbocz and Hol (1989) at $\bar{Z}$ values where there are (nearly) simultaneous buckling modes. At the higher $\bar{Z}$ values the fluctuation of $\bar{b} = \alpha^2 b$

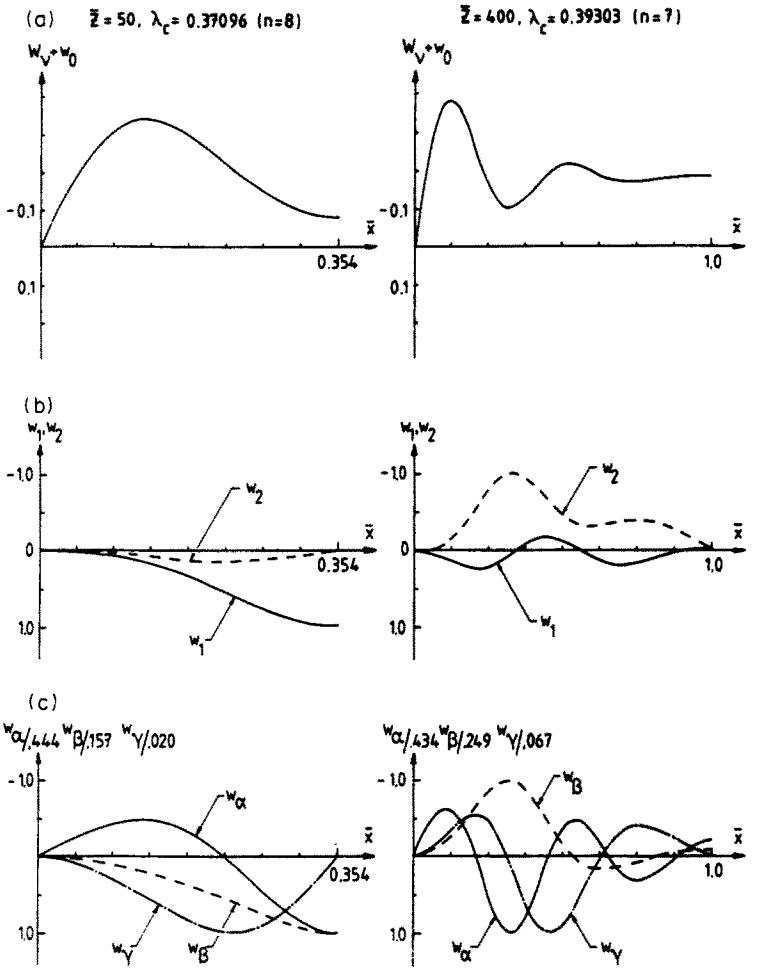

Fig. 10. Mode shapes of simply supported anisotropic shells under axial compression: (a) pre-buckling shapes, (b) buckling modes, (c) post-buckling modes.

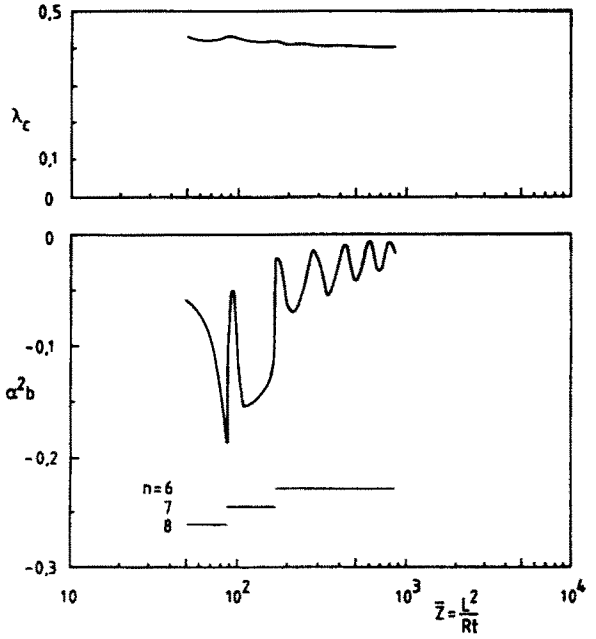

Fig. 11. Perfect shells buckling loads and imperfection sensitivity coefficients for fully clamped-anisotropic shells under axial compression.

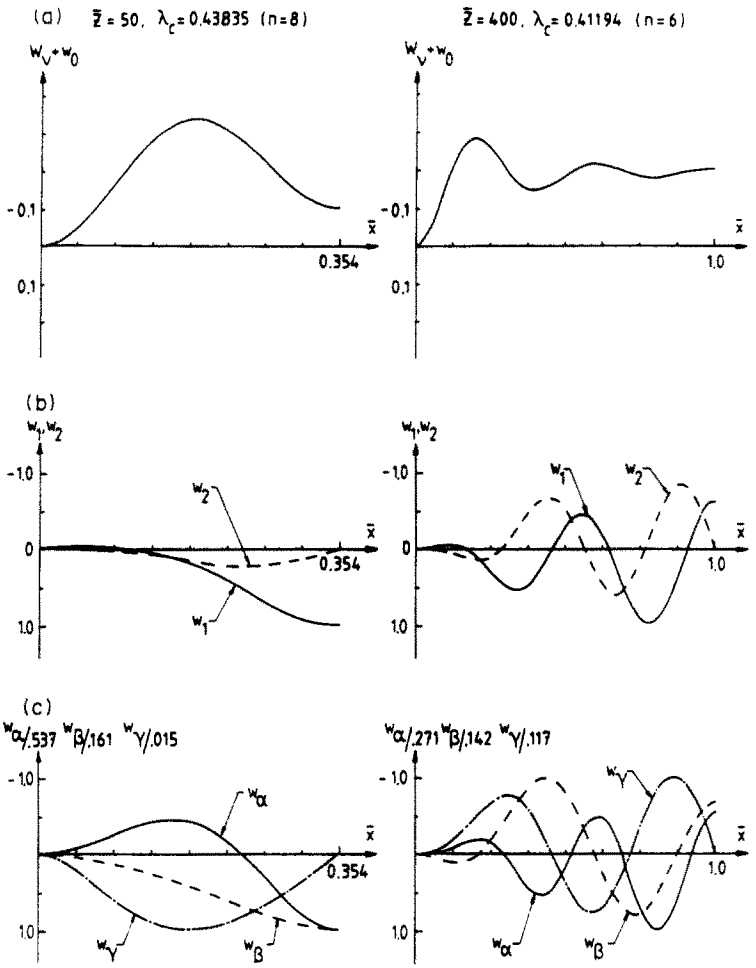

Fig. 12. Mode shapes of fully clamped anisotropic shells under axial compression: (a) pre-buckling shapes, (b) buckling modes, (c) post-buckling modes.

can be attributed to the minimization of λ_c with respect to discrete values of n. In Fig. 12 the pre-buckling, buckling and post-buckling mode shapes are displayed for shells of $\bar{Z} = 50$ and $\bar{Z} = 400$, respectively.

Hydrostatic pressure

For simply supported anisotropic shells the normalized buckling pressure $\bar{p}_c$ and the second imperfection sensitivity coefficient $\bar{b} = \alpha^2 b$ are shown in Fig. 13, whereas in Fig. 14 the pre-buckling, buckling and post-buckling mode shapes for shells of $\bar{Z} = 50$ and $\bar{Z} = 400$ are displayed. Notice that for $\bar{Z} = 50$ the w_γ-mode undergoes rapid changes close to the shell edge, a behaviour that would be missed completely by a coarse finite element discretization (Byskov, 1988). The decrease in $\bar{b} = \alpha^2 b$ with increasing values of $\bar{Z}$ is similar to earlier results obtained by Yamaki (1984) for isotropic shells. Notice that discontinuities in $\bar{b} = \alpha^2 b$ occur at places where there is a change in the critical circumferential wave number n. Also, a closer observation of Fig. 14 reveals that for the hydrostatic pressure loading both the buckling and the post-buckling modes are dominated by the cos $n\theta$ and cos $2n\theta$ terms thus exhibiting very little skewedness.

Counter-clockwise vs clockwise torsion

For the particular Booton shell chosen the only "16" and "26" terms in the constitutive equations listed in Table 3 that do not vanish are the $\bar{B}^*_{16}$ and $\bar{B}^*_{26}$ terms. These terms represent coupling between the bending and shear strain of the middle surface. Further, as can be seen from the constitutive equations, if the twisting of the cylinder is due to a positive

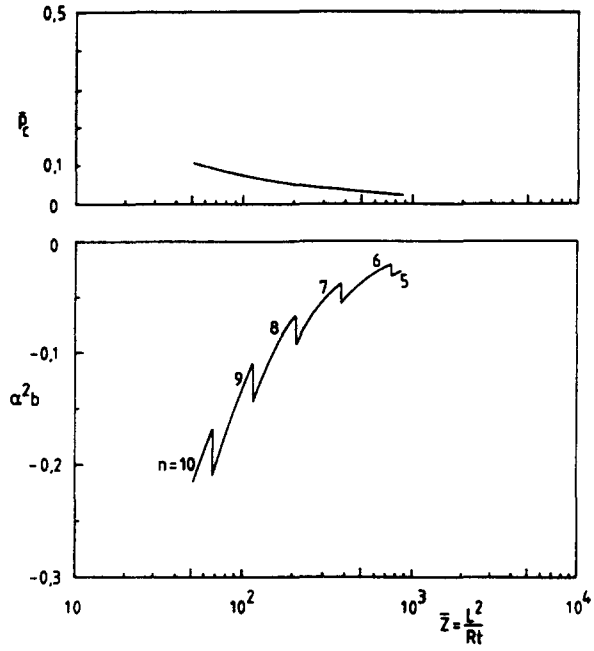

Fig. 13. Perfect shell buckling loads and imperfection sensitivity coefficients for simply supported anisotropic shells under hydrostatic pressure.

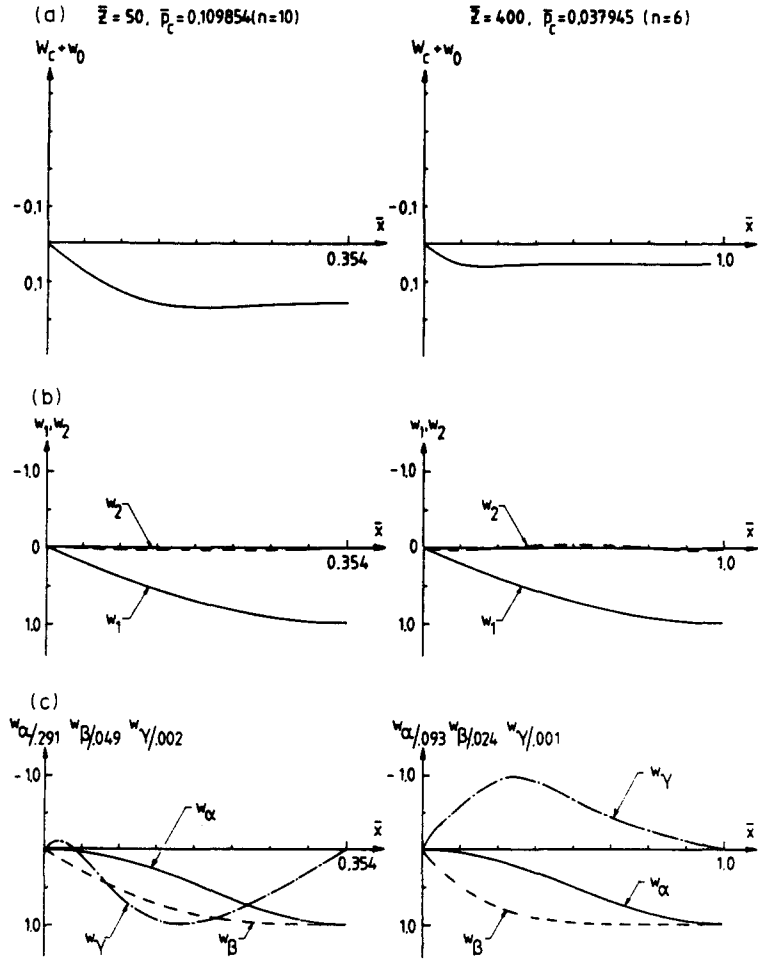

Fig. 14. Mode shapes of simply supported anisotropic shells under hydrostatic pressure: (a) pre-buckling shapes, (b) buckling modes, (c) post-buckling modes.

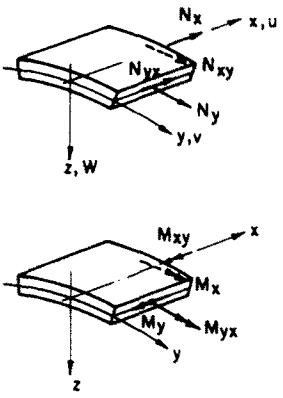

Fig. 15. Definition of stress- and moment resultants.

(counter-clockwise) applied torque, then γ_{xy} is also positive, which results in a negative bending moment M_x. Considering the definition of M_x in Fig. 15 it is clear that a negative bending moment will produce an outward normal deflection at the mid-plane of the shell (at $\bar{x} = 1/2(x/L)$), which is stabilizing (Hutchinson and Frauenthal, 1969). Conversely, a negative torsional loading (clockwise torque) results in a positive bending moment M_x, which in turn produces an inward normal deflection at $\bar{x} = 1/2(x/L)$, which is destabilizing. Considering now Figs 16 and 17, which display the pre-buckling, the buckling and the post-

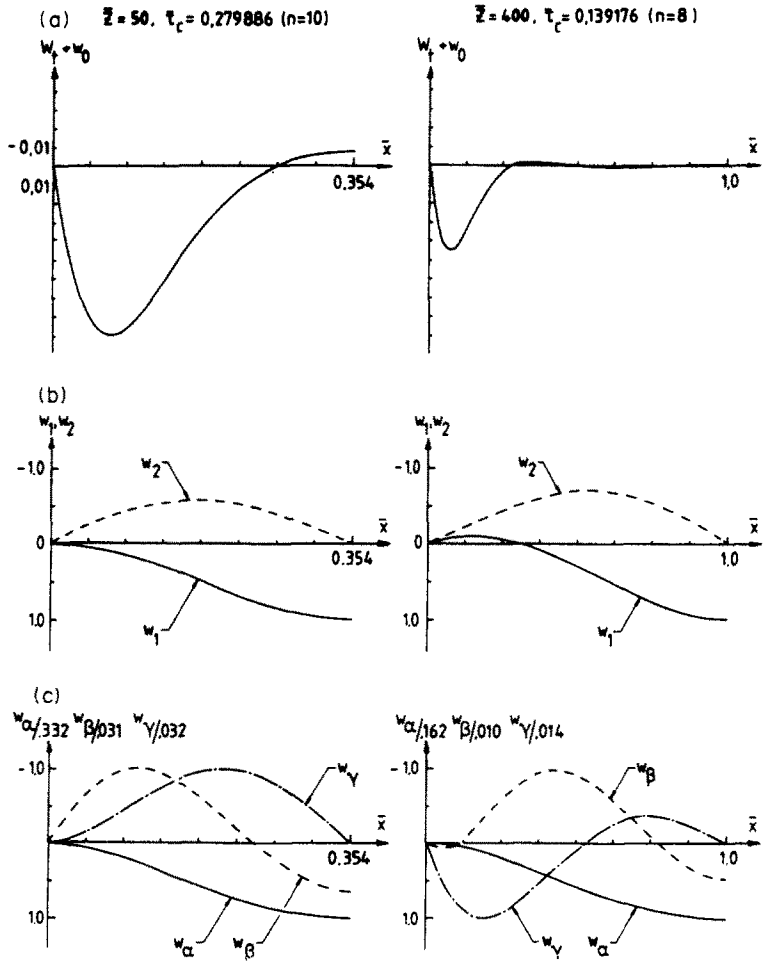

Fig. 16. Mode shapes for simply supported anisotropic shells under counter-clockwise torsion: (a) pre-buckling shapes, (b) buckling modes, (c) post-buckling modes.

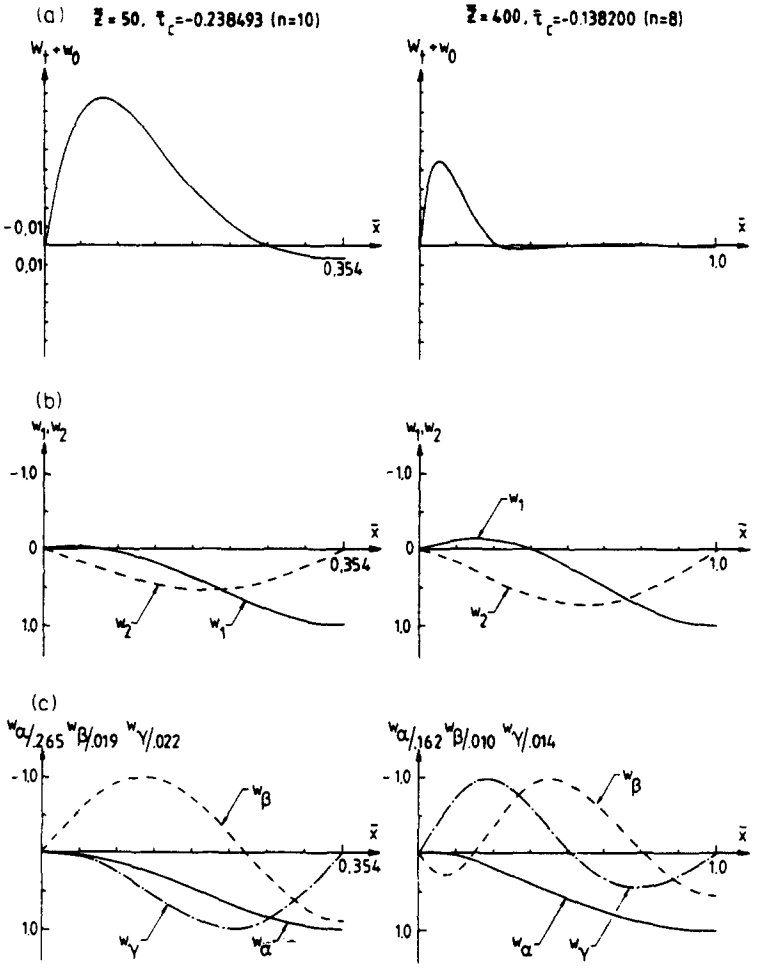

Fig. 17. Mode shapes for simply supported anisotropic shells under clockwise torsion: (a) pre-buckling shapes, (b) buckling modes, (c) post-buckling modes.

buckling modes for counter-clockwise ($\bar{\tau}_c > 0$) and clockwise ($\bar{\tau}_c < 0$) torsion, respectively, indeed the magnitudes (absolute values) of the critical normalized torsion parameter $\bar{\tau}_c$ are higher if the applied external torque is counter-clockwise. This phenomenon was first described by Booton (1976). Notice also that for torsional loading the pre-buckling deformations at the bifurcation point are about an order of magnitude smaller than for the other external loads considered.

From the plots of the second imperfection sensitivity coefficient $\bar{b} = \alpha^2 b$, shown in Figs 18 and 19, it is clear that for shorter shells ($\bar{Z} < 100$) if the applied torque is counter-clockwise one obtains a configuration which is more sensitive to initial imperfections affine to the buckling mode than if the applied external torque is clockwise. For increasing $\bar{Z} = L^2/Rt$ values the difference in imperfection sensitivity is smaller and the curves become gradually nearly identical and thus independent of the direction of the applied torque. Notice also that discontinuities in $\bar{b} = \alpha^2 b$ occur only at places where there is a change in the critical circumferential wave number n.

Experimental evidence (Arbocz and Babcock, 1969; Singer *et al.*, 1971), indicates that the shapes of the dominant initial imperfections in real structures often do not coincide with the buckling modes of the perfect structure. With the introduction of the imperfection form factors α and β the computational module ANILISA can also be used for an estimate of the imperfection sensitivity due to the occurrence of any single mode asymmetric imperfection. To illustrate this capability Tables 4 and 5 display data about the imperfection sensitivity of Booton's anisotropic shells under different external loads, whereby besides an initial imperfection *affine* to the respective buckling mode [see eqn (89)], the following *modal*

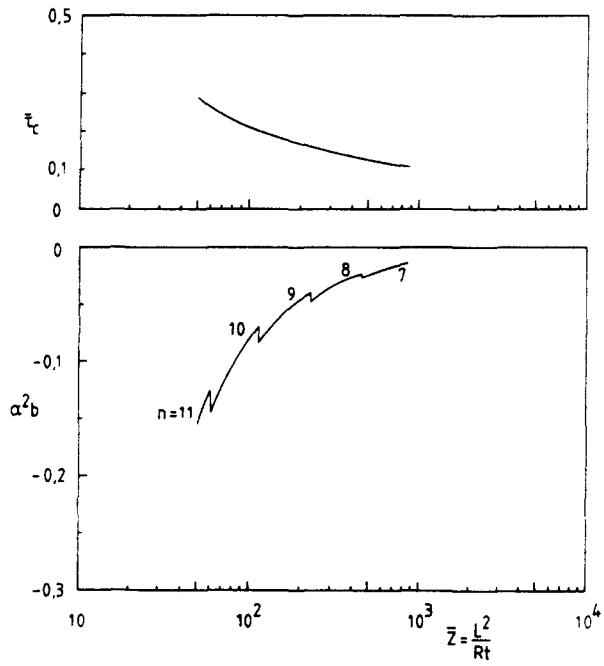

Fig. 18. Perfect shell buckling loads and imperfection sensitivity coefficients for simply supported anisotropic shells under counter-clockwise torsion.

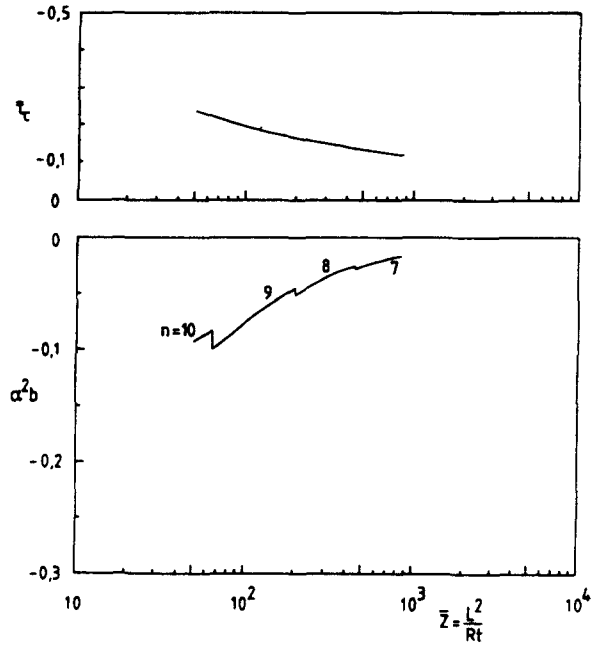

Fig. 19. Perfect shell buckling loads and imperfection sensitivity coefficients for simply supported anisotropic shells under clockwise torsion.

initial imperfection

$$\bar{W} = \bar{\xi}\hat{W} = \bar{\xi}t \sin(\pi x/L) \cos n\theta \tag{90}$$

has also been investigated. In all cases the circumferential wave number n is chosen to be identical to the critical wave number (the circumferential wave number at which the lowest buckling load occurs). Notice also that the *modal* imperfection specified by eqn (90) consists of a single half-wave in the axial direction.

Table 4. Imperfection form factors and imperfection sensitivity coefficients for axially compressed anisotropic shells

	Simply supported				Clamped			
	α		$\bar{b} = \alpha^2 b$		α		$\bar{b} = \alpha^2 b$	
$\bar{Z}$	Affine	Modal	Affine	Modal	Affine	Modal	Affine	Modal
50	0.4317	0.2743	−0.0685	−0.0277	0.4585	0.2092	−0.0573	−0.0119
100	0.4244	0.1462	−0.0585	−0.0069	0.9071	−0.0117	−0.0879	−0.0
200	0.4952	0.1155	−0.0680	−0.0037	0.9589	−0.0035	−0.0599	−0.0
300	0.5087	−0.0097	−0.0923	−0.0	0.9804	0.0133	−0.0102	−0.0
400	0.4804	0.0047	−0.0846	−0.0	0.9732	0.0077	−0.0326	−0.0
500	0.5060	−0.0025	−0.0886	−0.0	0.9811	0.0027	−0.0357	−0.0
600	0.4883	−0.0015	−0.0816	−0.0	0.9895	0.0037	−0.0096	−0.0
700	0.5022	0.0056	−0.0838	−0.0	0.9878	0.0021	−0.0279	−0.0
800	0.4977	0.0052	−0.0824	−0.0	0.9915	0.0012	−0.0102	−0.0
900	0.5022	0.0144	−0.0851	−0.0001	0.9937	0.0019	−0.0147	−0.0

Considering now the tabulated results it appears that for axial compression, except for shorter shells, the modal imperfection specified in eqn (90) does not affect the buckling load of the perfect anisotropic shells at all. On the other hand, if the external load is hydrostatic pressure then both the single affine and the single modal imperfections, specified by eqns (89) and (90), produce about the same degree of imperfection sensitivity. Further, also under counter-clockwise or clockwise torsional loading the single modal imperfection appears to cause very little imperfection sensitivity.

Finally, in the practice, the design engineers are not only interested in whether and how much the buckling load prediction of their proposed shell structure is sensitive to initial imperfections, they also want to obtain an estimate of the "knockdown" factor γ with which they must multiply the buckling load prediction of the perfect structure in order to arrive at the safe allowable load level. With the help of eqn (59) such an estimate can be computed if besides the imperfection sensitivity coefficient $\bar{b} = \alpha^2 b$ one also has an idea of the size of the amplitude $\bar{\xi}$ of the single mode imperfection that is likely to occur. For such cases the predictions of Cohen's formula [eqn (59)] are conveniently summarized in Fig. 20.

6. CONCLUSIONS

It is by now widely accepted that Koiter's General Theory of Elastic Stability (1967) has greatly contributed to our understanding of the sometimes perplexing stability behaviour of thin-walled structures. However, due to its mathematical complexity it is not always easy for the practising structural engineer to find the information he wants for the particular

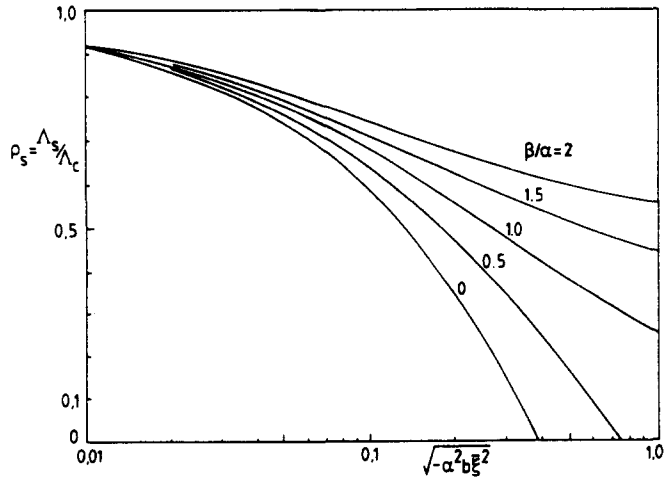

Fig. 20. Estimates of critical loads for imperfection sensitive structures (Cohen, 1971).

Table 5. Imperfection form factors and imperfection sensitivity coefficients for simply supported anisotropic shells

	Hydrostatic pressure				Counter-clockwise torsion				Clockwise torsion			
	α		$\bar{b} = \alpha^2 b$		α		$\bar{b} = \alpha^2 b$		α		$b = \alpha^2 b$	
$\bar{Z}$	Affine	Modal	Affine	Modal	Affine	Modal	Affine	Modal	Affine	Modal	Affine	Modal
50	0.9701	0.9519	−0.2157	−0.2077	1.0241	0.4344	−0.1542	−0.0277	1.0086	0.3974	−0.0906	−0.0141
100	0.9914	0.9761	−0.1289	−0.1250	1.0136	0.4085	−0.0811	−0.0132	1.0029	0.3771	−0.0760	−0.0108
200	0.9975	0.9915	−0.0669	−0.0661	1.0065	0.3823	−0.0454	−0.0066	1.0007	0.3311	−0.0445	−0.0049
300	0.9982	0.9953	−0.0522	−0.0519	1.0046	0.3908	−0.0352	−0.0053	1.0000	0.3510	−0.0351	−0.0043
400	0.9989	0.9967	−0.0509	−0.0507	1.0030	0.3585	−0.0261	−0.0033	0.9999	0.3243	−0.0269	−0.0028
500	0.9993	0.9977	−0.0361	−0.0360	1.0028	0.3982	−0.0244	−0.0038	0.9997	0.3730	−0.0246	−0.0034
600	0.9995	0.9982	−0.0271	−0.0270	1.0021	0.3793	−0.0200	−0.0029	0.9997	0.3571	−0.0205	−0.0026
700	0.9997	0.9985	−0.0211	−0.0210	1.0017	0.3603	−0.0170	−0.0022	0.9998	0.3407	−0.0176	−0.0020
800	0.9996	0.9987	−0.0283	−0.0283	1.0014	0.3416	−0.0148	−0.0017	0.9998	0.3242	−0.0154	−0.0016
900	0.9997	0.9989	−0.0234	−0.0234	1.0011	0.3232	−0.0131	−0.0014	0.9998	0.3077	−0.0138	−0.0013

structure at hand from the many publications that are available. What he needs is a computational module that enables him to obtain the desired information readily.

It has been shown that within the context of Koiter's initial post-buckling theory the computational module ANILISA can be used successfully to investigate the imperfection sensitivity of the buckling loads of isotropic, orthotropic and of fully anisotropic cylindrical shells under combined axial compression, external or internal pressure and torsion, taking into account the effect of different boundary conditions and of different initial imperfection shapes.

As a "building block" of the hierarchical design and analysis system "DISDECO" the computational module ANILISA makes feasible the first step towards acquiring detailed understanding of the expected instability behaviour of different cylindrical shell configurations. This knowledge is a prerequisite for the development of discrete nonlinear computational models which can reliably predict the load carrying capability of the structure.

It must be stressed that the predictions of ANILISA provide only a first indication of the expected nonlinear behaviour and all its findings must be evaluated within the context of the fundamental assumptions involved in the theory. Thus the fact that a single long wavelength modal imperfection does not appear to produce any significant imperfection sensitivity may be misleading, since especially under axial compression for the anisotropic shells considered there may exist several nearly simultaneous buckling modes, and it is known that in such situations nonlinear modal interaction may reduce the load carrying capability of the structure considerably. For these cases the user must switch to other more advanced computational modules available within "DISDECO" which can handle the nonlinear interaction problem of multiple initial imperfection and response modes.

Acknowledgement—This paper is dedicated to the memory of Charles Dwight Babcock Jr, a longtime friend and colleague, whose untimely death has deeply saddened all those who have known him. The authors wish to thank Mrs. Annemarie van Lienden-Datema for the skilful typing of the manuscript and Mr. B. van Wimersma Greidanus for the fine artwork. Special thanks are due to SUN Microsystems Nederland B.V. for their support of the development of "DISDECO" via the donation of a SUN 3/140 workstation.

REFERENCES

Almroth, B. O. (1966). Influence of imperfections and edge restraint on the buckling of axially compressed cylinders. NASA CR-432.

Anonymous (1977). *Rules for the Design, Construction and Inspection of Offshore Structures*. DnV (Det norske Veritas), Oslo, Norway.

Anonymous (1980). Beulsicherheitsnachweise für Schalen, DASt Richtlinie 013. Deutscher Ausschuss für Stahlbau.

Anonymous (1984). ESA software engineering standards. ESA BSSC (84) 1.

Arbocz, J. and Babcock, C. D. Jr. (1969). The effect of general imperfections on the buckling of cylindrical shells. *ASME J. Appl. Mech.* **36**, 28–38.

Arbocz, J. and Babcock, C. D. Jr. (1980). The buckling analysis of imperfection sensitive shell structures. NASA CR-3310.

Arbocz, J. and Hol, J. M. A. M. (1989). ANILISA—Computational module for Koiter's imperfection sensitivity theory. Report LR-582, Delft University of Technology, the Netherlands.

Arbocz, J. and Sechler, E. E. (1974). On the buckling of axially compressed imperfect cylindrical shells. *ASME J. Appl. Mech.* **41**, 737–743.

Arbocz, J. and Sechler, E. E. (1976). On the buckling of stiffened imperfect cylindrical shells. *AIAA Jl* **14**(11), 1611–1617.

Ashton, J. E., Halpin, J. C. and Petit, P. H. (1969). *Primer on Composite Materials: Analysis*. Technomic Publishing Co., Stamford, Connecticut.

Booton, M. (1976). Buckling of imperfect anisotropic cylinders under combined loading. UTIAS Report No. 203, University of Toronto.

Budiansky, B. (1965). Dynamic buckling of elastic structures: criteria and estimates. *Proc. Int. Conf. Dynamic Stability of Structures*, pp. 83–106. Pergamon Press, Oxford.

Budiansky, B. and Hutchinson, J. W. (1964). Dynamic buckling of imperfection sensitive structures. *Proc. 11th IUTAM Congress*, pp. 636–651. Springer-Verlag, Berlin/Göttingen/Heidelberg/New York.

Bushnell, D. (1972). Stress, stability and vibration of complex branched shells of revolution: Analysis and user's manual for BOSOR-4. NASA CR-2116.

Byskov, E. (1988). Smooth postbuckling stresses by a modified finite element method. DCAMM Report No. 380, Technical University of Denmark.

Byskov, E. and Hutchinson, J. W. (1977). Mode interaction in axially stiffened cylindrical shells. *AIAA Jl* **15**(7), 941–948.

Cohen, G. A. (1968). Effect of a nonlinear prebuckling state on the postbuckling behavior and imperfection sensitivity of elastic structures. *AIAA Jl* **6**(8), 1616–1619.
Cohen, G. A. (1971). Computer program for analysis of imperfection sensitivity of ring-stiffened shells of revolution. NASA CR-1801.
Cohen, G. A. (1968). Computer analysis of asymmetric buckling of ring-stiffened orthotropic shells of revolution. *AIAA Jl* **6**(1), 141–149.
Elishakoff, I. and Arbocz, J. (1985). Reliability of axially compressed cylindrical shells with general nonsymmetric imperfections. *ASME J. Appl. Mech.* **52**, 122–128.
Elishakoff, I., Van Manen, S., Vermeulen, P. G. and Arbocz, J. (1987). First-order second-moment analysis of the buckling of shells with random imperfections. *AIAA Jl* **25**(8), 1113–1117.
Fitch, J. R. (1968). The buckling and post-buckling behavior of spherical caps under concentrated load. *Int. J. Solids Structures* **4**, 421–446.
Hol, J. M. A. M. (1989). Layout and design of the preliminary version of DISDECO. Report LR-577, Delft University of Technology, the Netherlands.
Hutchinson, J. W. and Amazigo J. C. (1967). Imperfection sensitivity of eccentrically stiffened cylindrical shells. *AIAA Jl* **5**(3), 392–401.
Hutchinson, J. W. and Frauenthal, J. C. (1969). Elastic postbuckling behavior of stiffened and barreled cylindrical shells. *ASME J. Appl. Mech.* **36**, 784–790.
Keller, H. (1968). *Numerical Methods of Two-Point Boundary Value Problems*. Blaisdell Publishing Co., Waltham, Mass.
Koiter, W. T. (1967). On the stability of elastic equilibrium. Ph.D. Thesis, in Dutch, TH-Delft, the Netherlands. H.T. Paris, Amsterdam 1945. English translation issued as NASA TTF-10, 833 pp.
Liu, D. K. (1988). Nonlinear vibrations of imperfect thin-walled cylindrical shells. Ph.D. Thesis, Faculty of Aerospace Engineering, Delft University of Technology, the Netherlands.
Singer, J., Arbocz, J. and Babcock, C. D. Jr. (1971). Buckling of imperfect stiffened cylindrical shells under axial compression. *AIAA Jl* **9**(1), 68–75.
Tennyson, R. C., Booton, M. and Chan, K. H. (1978). Buckling of short cylinders under combined loading. *ASME J. Appl. Mech.* **45**, 574–578.
Tennyson, R. C. and Muggeridge, D. B. (1969). Buckling of axisymmetric imperfect circular cylindrical shells under axial compression. *AIAA Jl* **7**(11), 2127–2131.
Vermeulen, P. G. (1982). Stability of an anisotropic cylindrical shell under axial compression. Ir. Thesis (in Dutch), Faculty of Aerospace Engineering, Delft University of Technology, the Netherlands.
Von Kármán, T. and Biot, M. A. (1940). *Mathematical Methods in Engineering*, p. 317. McGraw-Hill Book Co., New York.
Weingarten, V. I., Morgan, E. J. and Seide, P. (1965). Elastic stability of thin-walled cylindrical and conical shells under axial compression. *AIAA Jl* **3**(3), 500–505.
Yamaki N. (1984). *Elastic Stability of Circular Cylindrical Shells*. North-Holland Series in Applied Mathematics and Mechanics, Vol. 27. Elsevier Science Publishers BV, Amsterdam, the Netherlands.

APPENDIX A

Periodicity condition

If the solution is to satisfy the periodicity requirement then, by definition

$$\int_0^{2\pi R} v_{,y}\,\mathrm{d}y = 0 \tag{A1}$$

must hold where

$$v_{,y} = \varepsilon_y + (1/R)W - (1/2)W_{,y}^2 \tag{A2}$$

$$\varepsilon_y = A_{12}^* N_x + A_{22}^* N_y + A_{26}^* N_{xy} + B_{21}^* \kappa_x + B_{22}^* \kappa_y + B_{26}^* \kappa_{xy} \tag{A3}$$

further

$$N_x = F_{,yy}, \qquad N_y = F_{,xx}, \qquad N_{xy} = -F_{,xy}$$

and

$$\kappa_x = -W_{,xx}, \quad \kappa_y = -W_{,yy}, \quad \kappa_{xy} = -2W_{,xy}.$$

Substituting for W and F the assumed perturbation expansion yields after regrouping and ordering by powers of ξ

$$\begin{aligned}
v_{,y} = {} & (t/cR)\{(-\lambda\bar{A}_{12}^* + cW_v) + (-\bar{p}\bar{A}_{22}^* + cW_p) + (\bar{\tau}\bar{A}_{26}^* + cW_t) + \bar{A}_{22}^* f_0'' - (t/2R)\bar{B}_{21}^* w_0'' + cw_0\} \\
& + (t/cR)\xi\{[\bar{A}_{22}^* f_1'' - \bar{A}_{12}^* n^2 f_1 - \bar{A}_{26}^* n f_2' - (t/2R)(\bar{B}_{21}^* w_1'' - \bar{B}_{22}^* n^2 w_1 + 2\bar{B}_{26}^* n w_2') + cw_1]\cos n\theta \\
& + [\bar{A}_{22}^* f_2'' - \bar{A}_{12}^* n^2 f_2 + \bar{A}_{26}^* n f_1' - (t/2R)(\bar{B}_{21}^* w_2'' - \bar{B}_{22}^* n^2 w_2 - 2\bar{B}_{26}^* n w_1') + cw_2]\sin n\theta\} \\
& + (t/cR)\xi^2\{\bar{A}_{22}^* f_\alpha'' - (t/2R)\bar{B}_{21}^* w_\alpha'' + cw_\alpha - (ct/4R)n^2(w_1^2 + w_2^2) + \cdots + [\bar{A}_{22}^* f_\beta'' - \bar{A}_{12}^* 4n^2 f_\beta - \bar{A}_{26}^* 2n f_\gamma' \\
& - (t/2R)(\bar{B}_{21}^* w_\beta'' - \bar{B}_{22}^* 4n^2 w_\beta + 4\bar{B}_{26}^* n w_\gamma') + cw_\beta + (ct/4R)n^2(w_1^2 - w_2^2)]\cos 2n\theta \\
& + [\bar{A}_{22}^* f_\gamma'' - \bar{A}_{12}^* 4n^2 f_\gamma + \bar{A}_{26}^* 2n f_\beta'
\end{aligned}$$

$$-(t/2R)(\bar{B}^*_{21}w''_\gamma - \bar{B}^*_{22}4n^2w_\gamma - 4\bar{B}^*_{26}nw'_\beta) + cw_\gamma + (ct/2R)n^2w_1w_2]\sin 2n\theta\}$$
$$+(t/cR)\xi^3\{-(ct/R)n^2[(w_1w_\beta + w_2w_\gamma)\cos n\theta - (w_2w_\beta - w_1w_\gamma)\sin n\theta$$
$$-(w_1w_\beta - w_2w_\gamma)\cos 3n\theta - (w_2w_\beta + w_1w_\gamma)\sin 3n\theta]\}$$
$$+(t/cR)\xi^4\{-(ct/R)n^2[w_\beta^2 + w_\gamma^2 - 2w_\beta w_\gamma\sin 4n\theta - (w_\beta^2 - w_\gamma^2)\cos 4n\theta]\} \tag{A4}$$

where $\theta = y/R$. Substituting this expression into eqn (A1) and carrying out the y-integration yields

$$\{(-\lambda\bar{A}^*_{12} + cW_v) + (-\bar{p}\bar{A}^*_{22} + cW_p) + (\bar{\tau}\bar{A}^*_{26} + cW_t) + \underline{\bar{A}^*_{22}f''_0 - (t/2R)\bar{B}^*_{21}w''_0 + cw_0}\}$$
$$+\xi^2\{\underline{\bar{A}^*_{22}f''_2 - (t/2R)\bar{B}^*_{21}w''_2 + cw_2 - (ct/4R)n^2(w_1^2 + w_2^2)}\} + \xi^4\{-(ct/R)n^2(w_\beta^2 + w_\gamma^2)\} = 0. \tag{A5}$$

Notice that the underlined terms vanish identically since they are equal to eqns (15) and (34), respectively, with the constants $\bar{C}_1 = \bar{C}_2 = 0$ and $\bar{C}_3 = \bar{C}_4 = 0$. If one now lets

$$W_v = \bar{A}^*_{12}\lambda/c \tag{A6a}$$
$$W_p = \bar{A}^*_{22}\bar{p}/c \tag{A6b}$$
$$W_t = -\bar{A}^*_{26}\bar{\tau}/c \tag{A6c}$$

then the periodicity condition (A1) is satisfied up to and including terms of the order ξ^3.